N-Heterocyclic Carbene Stabilized *trans*-Dihydrido Aqua and Ethanol Complexes of Ruthenium: Precursors to Complexes with Ru−Heteroatom Bonds

Rodolphe F. R. Jazzar, Purvi H. Bhatia, Mary F. Mahon, and Michael K. Whittlesey*

Department of Chemistry, University of Bath, Claverton Down, Bath BA2 7AY, U.K.

Received August 20, 2002

Attempts to isolate the bis-N-heterocyclic carbene complex $Ru(AsPh_3)(IMes)_2(CO)H_2$ (IMes = bis(1,3-(2,4,6-trimethylphenyl)imidazol-2-ylidene)) by crystallization with either ethanol or hexane yields instead the ethanol and water complexes $Ru(IMes)_2(CO)(EtOH)H_2$ (**1**) and $Ru(IMes)_2(CO)(H_2O)H_2$ (**2**), respectively. Both multinuclear NMR spectroscopy and X-ray crystallography demonstrate that these two compounds are isostructural with a *trans* arrangement of the hydride ligands. Thermolysis of **1** results in decarbonylation of the bound ethanol ligand to yield $Ru(IMes)_2(CO)_2H_2$ (**3**). Substitution of the coordinated solvent ligands in **1** or **2** occurs readily with *p*-ethoxyphenol to give $Ru(IMes)_2(CO)(HOC_6H_4$-*p*-$OEt)H_2$ (**4**), while treatment of **2** with 1-propanethiol affords the thiol complex $Ru(IMes)_2(CO)(HSCH_2CH_2CH_3)H_2$ (**8**). Reaction of **8** with CO gives the thiolate hydride species $Ru(IMes)_2(CO)_2(SCH_2CH_2CH_3)H$ (**9**), whereas addition of CO to either **1** or **2** affords $Ru(IMes)_2(CO)_3$ (**5**). The hydroxy hydride complex $Ru(IMes)_2(CO)_2(OH)H$ (**6**) has been isolated as an intermediate on the pathway from **2** to **5**. Addition of CO_2 or *p*-$HO_2CC_5H_4N$ to solutions of **2** yields the bicarbonate complex $Ru(IMes)_2(CO)(\kappa^2$-$O_2COH)H$ (**10**) and the isonicotinate species $Ru(IMes)_2(CO)(\kappa^2$-$O_2CC_5H_4N)H$ (**11**), respectively. Addition of CO to **10** affords $Ru(IMes)_2(CO)_2(\eta^1$-$O_2COH)H$ (**7**). Treatment of complex **2** with excess acetonitrile yields the *N*-imidoylimidato complex $Ru(IMes)_2(CO)(NH{=}C(CH_3)N{=}C(CH_3)O)H$ (**12**), which arises from the formal addition of two molecules of acetonitrile in head-to-tail fashion across the RuO−H bond. Compounds **1**, **2**, **6**, **7**, **8**, **9**, **11**, and **12** have been structurally characterized by single-crystal X-ray diffraction.

Introduction

Complexes containing bonds between late transition metals and heteroatoms such as nitrogen, oxygen, and sulfur have been identified as playing key roles in both biological processes[1] (e.g., Fe−S in nitrogenase, Fe−OH in lipoxygenase) and catalytic reactions, such as alkene oxidation (Wacker process)[2] and hydroamination.[3] For second- and third-row metals, hard−soft acid−base (HSAB) theory predicts an energetic mismatch between the "soft" metal and "hard" anionic N and O ligands, which imparts the resulting metal alkoxo, hydroxo, and amido complexes with exceptionally interesting physical and chemical properties.[4] For example, the hydroxo and parent amido complexes *trans*-$Ru(dmpe)_2(OH)H$ and *trans*-$Ru(dmpe)_2(NH_2)H$ display remarkable basicities (estimated pK_a values of the protonated complexes of ca. 22 and 32, respectively),[5] while C_2H_4 insertion into the Ir−OH bond in $Cp^*Ir(PMe_3)Ph(OH)$ occurs under unexpectedly mild conditions.[6]

In recent years, there has been an increase in the number of examples of well-characterized M−X (X = O, N) complexes, with the development of more general and reliable routes to their synthesis.[7] This has allowed structure/bonding/reactivity relationships, the role of pπ−dπ interactions, correlation of M−X and H−X bond strengths, and fundamental chemical reactivity toward organic substrates to be studied in more detail.[8] Much of this work has utilized complexes containing carbocy-

* Corresponding author. E-mail: chsmkw@bath.ac.uk

(1) Holm, R. H.; Kennepohl, P.; Solomon, E. I. *Chem. Rev.* **1996**, *96*, 2239, and references therein.

(2) (a) Bäckvall, J. E.; Akermark, B.; Ljunggren, S. O. *J. Am. Chem. Soc.* **1979**, *101*, 2411. (b) Bäckvall, J. E.; Bjorkmann, E. E.; Pettersson, L.; Siegbahn, P. *J. Am. Chem. Soc.* **1984**, *106*, 4369. (c) Bäckvall, J. E.; Bjorkmann, E. E.; Pettersson, L.; Siegbahn, P. *J. Am. Chem. Soc.* **1985**, *107*, 7265.

(3) (a) Müller, T. E.; Beller, M. *Chem. Rev.* **1998**, *98*, 675. (b) Johnson, J. S.; Bergman, R. G. *J. Am. Chem. Soc.* **2001**, *123*, 2923.

(4) Bryndza, H. E.; Tam, W. *Chem. Rev.* **1988**, *88*, 1163.

(5) Fulton, J. R.; Bouwkamp, M. W.; Bergman, R. G. *J. Am. Chem. Soc.* **2000**, *122*, 8799. Fulton, J. R.; Sklenak, S.; Bouwkamp, M. W.; Bergman, R. G. *J. Am. Chem. Soc.* **2002**, *124*, 4722.

(6) Woerpel, K. A.; Bergman, R. G. *J. Am. Chem. Soc.* **1993**, *115*, 7888.

(7) For reviews, see: (a) Bergman, R. G. *Polyhedron* **1995**, *14*, 3227. (b) Sharp, P. R. *Comments Inorg. Chem.* **1999**, *21*, 85. (c) Sharp, P. R. *J. Chem. Soc., Dalton Trans.* **2000**, 2647. For recent examples, see: (d) Hartwig, J. F.; Andersen, R. A.; Bergman, R. G. *J. Am. Chem. Soc.* **1989**, *111*, 2717. (e) Hartwig, J. F.; Andersen, R. A.; Bergman, R. G. *Organometallics* **1991**, *10*, 1875. (f) Blum, O.; Milstein, D. *J. Am. Chem. Soc.* **1995**, *117*, 4582. (g) VanderLende, D. D.; Abboud, K. A.; Boncella, J. M. *Inorg. Chem.* **1995**, *34*, 5319. (h) Driver, M. S.; Hartwig, J. F. *J. Am. Chem. Soc.* **1995**, *117*, 4708. (i) Holland, P. L.; Andersen, R. A.; Bergman, R. G. *J. Am. Chem. Soc.* **1996**, *118*, 1092. (j) Boncella, J. M.; Eve, T. M.; Rickman, B.; Abboud, K. A. *Polyhedron* **1998**, *17*, 725. (k) Kaplan, A. W.; Ritter; J. C. M.; Bergman, R. G. *J. Am. Chem. Soc.* **1998**, *120*, 6828. (l) Mann, G.; Incarvito, C.; Rheingold, A. L.; Hartwig, J. F. *J. Am. Chem. Soc.* **1999**, *121*, 3224. (m) Matsuzaka, H.; Kamura, T.; Ariga, K.; Watanabe, Y.; Okubo, T.; Ishii, T.; Yamashita, M.; Kondo, M.; Kitagawa, S. *Organometallics* **2000**, *19*, 216. (n) Jayaprakash, K. N.; Gunnoe, T. B.; Boyle, P. D. *Inorg. Chem.* **2001**, *40*, 6481. (o) Tejel, C.; Ciriano, M. A.; Bordonaba, M.; López, J. A.; Lahoz, F. J.; Oro, L. A. *Inorg. Chem.* **2002**, *41*, 2348.

10.1021/om020684e CCC: $25.00
Publication on Web 01/22/2003

clic rings (arene, cyclopentadienyl) and/or phosphines as ancillary ligands, and hence, the influence of steric and electronic factors on the chemistry of M−X bonds remains generally unexplored.

We have recently started to study the reactivity of simple mixed phosphine N-heterocyclic carbene (NHC) complexes of ruthenium. NHCs have been the focus of considerable interest in homogeneous catalysis as alternatives to tertiary phosphines,[9] although there are important differences between the two types of ligand. NHCs are very strong σ-donors but poor π-acceptors, while the effective two-dimensional structure of the heterocyclic ring contrasts with the ball structure of phosphines. Moreover, the carbene substituents are one bond further removed from the metal center compared to phosphines (eq 1), which, taken together with relative ease of introducing sterically demanding groups at the nitrogen atoms of the imidazol-2-ylidene skeleton,[10] affords the possibility of stabilizing coordinatively unsaturated, reactive metal centers,[11] or alternatively, favoring unusual coordination geometries and/or ancillary ligand sets.[12]

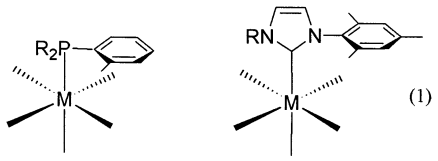

(1)

We have recently reported the unprecedented C−C bond activation of an unstrained sp^2−sp^3 hybridized C−C bond of the well-known carbene IMes (IMes = bis-(1,3-(2,4,6-trimethylphenyl)imidazol-2-ylidene)) upon reaction with $Ru(PPh_3)_3(CO)H_2$ (Scheme 1).[13]

Scheme 1

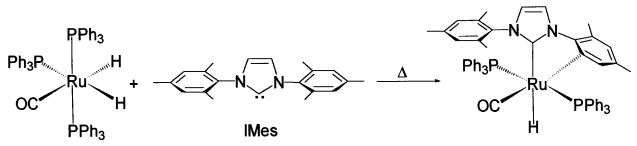

Scheme 2

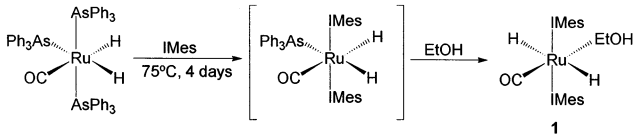

In an attempt to find milder conditions for this transformation, we have turned to the triphenylarsine precursor $Ru(AsPh_3)_3(CO)H_2$. This complex displays remarkably different reactivity toward IMes compared to the phosphine analogue, affording under the same reaction conditions *trans*-dihydride ethanol and water complexes of ruthenium devoid of arsine ligands and stabilized by the presence of two bulky NHC groups. The reactions of these complexes with a range of small molecules (CO, CO_2, CH_3CN) provides a route to stable products containing Ru−O and Ru−N linkages, including the hydroxy hydride $Ru(IMes)_2(CO)_2(OH)H$ and the *N*-imidoylimidato complex $Ru(IMes)_2(CO)(NH{=}C(CH_3)$-$N{=}C(CH_3)O)H$.

Results and Discussion

Formation and Characterization of $Ru(IMes)_2$-$(CO)(EtOH)H_2$ (1) and $Ru(IMes)_2(CO)(H_2O)H_2$ (2). The reaction of $Ru(AsPh_3)_3(CO)H_2$ with 3−4 equiv of IMes overnight at 75 °C afforded a mixture of unreacted starting material and the bis-carbene complex Ru-$(AsPh_3)(IMes)_2(CO)H_2$. None of the monosubstituted species $Ru(AsPh_3)_2(IMes)(CO)H_2$ was detectable by NMR. Continued heating for 4 days gave a solution containing only $Ru(AsPh_3)(IMes)_2(CO)H_2$, which displayed two doublets in the hydride region of the ^1H NMR spectrum (δ −5.71 and −8.93, J_{HH} = 5.9 Hz), consistent with the *cis*-RuH_2 stereochemistry shown in Scheme 2, and a single methyl resonance (δ 2.15) integrating in a ratio of 1:1:36. Two low-field resonances at δ 202.8 and 197.1 in the $^{13}C\{^1H\}$ NMR spectrum were assigned to the presence of Ru−*C*O and Ru−*C*(carbene), respectively.

Attempts to isolate this bis-carbene complex by crystallization from ethanol (a solvent that previously proved successful for crystallization of Ru phosphine/NHC complexes)[13] gave instead $Ru(IMes)_2(CO)(EtOH)$-H_2 (**1**), in which the triphenylarsine ligand had been displaced by ethanol (Scheme 2). Complex **1** was isolated in 78% yield as an air-sensitive yellow microcrystalline solid. The solid state structure of **1** was determined by X-ray crystallography and is shown in the ORTEX plot in Figure 1.[14] The geometry at ruthenium (Table 1) is close to octahedral with two *trans* IMes ligands (180.000-(1)°).

(8) (a) Bryndza, H. E.; Fong, L. K.; Paciello, R. A.; Tam, W.; Bercaw, J. E. *J. Am. Chem. Soc.* **1987**, *109*, 1444. (b) Poulton, J. T.; Folting, K.; Streib, W. E.; Caulton, K. G. *Inorg. Chem.* **1992**, *31*, 3190. (c) Caulton, K. G. *New. J. Chem.* **1994**, *18*, 25. (d) Holland, P. J.; Andersen, R. A.; Bergman, R. G.; Huang, J.; Nolan, S. P. *J. Am. Chem. Soc.* **1997**, *119*, 12800. (e) Holland, P. L.; Andersen, R. A.; Bergman, R. G. *Comments Inorg. Chem.* **1999**, *21*, 115. (f) Fulton, J. R.; Holland, A. W.; Fox, D. J.; Bergman, R. G. *Acc. Chem. Res.* **2002**, *35*, 44.

(9) There have been a number of definitive recent reviews on the properties of NHCs, their transition metal chemistry, and roles in homogeneous catalysis: (a) Bourissou, D.; Guerret, O.; Gabbaï, F. P.; Bertrand, G. *Chem. Rev.* **2000**, *10*, 39. (b) Weskamp, T.; Böhm, V. P. W.; Herrmann, W. A. *J. Organomet. Chem.* **2000**, *600*, 12. (c) Jafarpour, L.; Nolan, S. P. *J. Organomet. Chem.* **2001**, *617*−*618*, 17. (d) Jafarpour, L.; Nolan, S. P. *Adv. Organomet. Chem.* **2001**, *46*, 181. (e) Herrmann, W. A.; Weskamp, T.; Böhm, V. P. W. *Adv. Organomet. Chem.* **2002**, *48*, 1. (f) Herrmann, W. A. *Angew. Chem., Int. Ed.* **2002**, *41*, 1290.

(10) (a) Arduengo, A. J., III; Harlow, R. L.; Kline, M. *J. Am. Chem. Soc.* **1991**, *113*, 361. (b) Arduengo, A. J., III; Dias, H. V. R.; Harlow, R. L.; Kline, M. *J. Am. Chem. Soc.* **1992**, *114*, 5530. (c) Enders, D.; Breuer, K.; Raabe, G.; Runsink, J.; Teles, J. H.; Melder, J. P.; Ebel, K.; Brode, S. *Angew. Chem., Int. Ed. Engl.* **1995**, *34*, 1021. (d) Herrmann, W. A.; Elison, M.; Fischer, J.; Köcher, C.; Artus, G. R. *Chem. Eur. J.* **1996**, *2*, 772. (e) Herrmann, W. A.; Köcher, C.; Goossen, L. J.; Artus, G. R. *Chem. Eur. J.* **1996**, *2*, 1627. (f) Herrmann, W. A.; Goossen, L. J.; Artus, G. R. J.; Köcher, C. *Organometallics* **1997**, *16*, 2472. (g) Arduengo, A. J., III; Krafczyk, R.; Schmutzler, R.; Craig, H. A.; Goerlich, J. R.; Marshall, W. J.; Unverzagt, M. *Tetrahedron* **1999**, *55*, 14523. (h) Xu, L.; Chen, W.; Bickley, J. F.; Steiner, A.; Xiao, J. *J. Organomet. Chem.* **2000**, *598*, 409. (i) Jafarpour, L.; Stevens, E. D.; Nolan, S. P. *J. Organomet. Chem.* **2000**, *606*, 49. (j) Fürstner, A.; Ackermann, L.; Gabor, B.; Goddard, R.; Lehmann, C. W.; Mynott, R.; Stelzer, F.; Thiel, O. R. *Chem. Eur. J.* **2001**, *7*, 3236.

(11) (a) Louie, J.; Grubbs, R. H. *Chem. Commun.* **2000**, 1479. (b) Sandford, M. S.; Ulman, M.; Grubbs, R. H. *J. Am. Chem. Soc.* **2001**, *123*, 749. (c) Gstöttmayr, C. W. K.; Böhm, V. P. W.; Herdtweck, E.; Grosche, M.; Herrmann, W. A. *Angew. Chem., Int. Ed.* **2002**, *41*, 1363. (d) Cavallo, L. *J. Am. Chem. Soc.* **2002**, *124*, 8965.

(12) (a) Oldham, W. J., Jr.; Oldham, S. M.; Scott, B. L.; Abney, K. D.; Smith, W. H.; Costa, D. A. *Chem. Commun.* **2001**, 1348. (b) Gründemann, S.; Kovacevic, A.; Albrecht, M.; Faller, J. W.; Crabtree, R. H. *Chem. Commun.* **2001**, 2274. (c) Carlson, R. G.; Gile, M. A.; Heppert, J. A.; Mason, M. H.; Powell, D. R.; Velde, D. V.; Vilain, J. M. *J. Am. Chem. Soc.*, **2002**, *124*, 1580.

(13) Jazzar, R. F. R.; Macgregor, S. A.; Mahon, M. F.; Richards, S. P.; Whittlesey, M. K. *J. Am. Chem. Soc.*, **2002**, *124*, 4944.

(14) McArdle, P. *J. Appl. Crystallogr.* **1994**, *27*, 438.

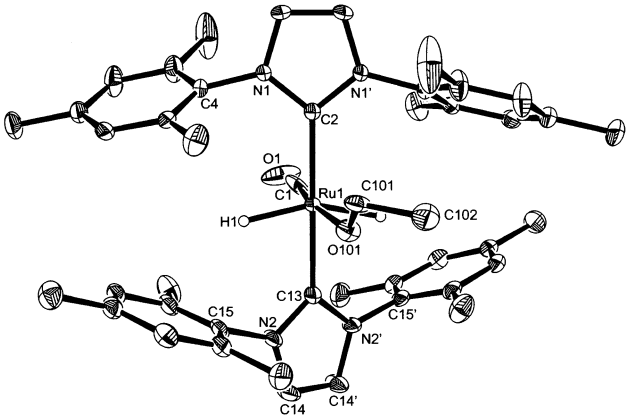

Figure 1. ORTEX diagram of $Ru(IMes)_2(CO)(EtOH)H_2$ (**1**). Thermal ellipsoids are shown at the 30% probability level.

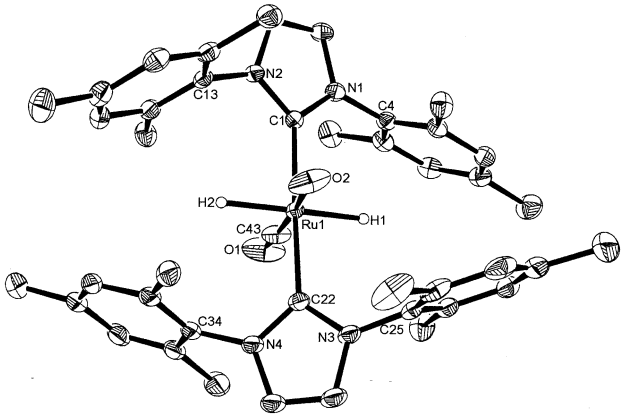

Figure 2. ORTEX diagram of $Ru(IMes)_2(CO)(H_2O)H_2$ (**2**). Thermal ellipsoids are shown at the 30% probability level.

Table 1. Selected Bond Lengths [Å] and Angles [deg] for $Ru(IMes)_2(CO)(EtOH)H_2$ (1)

Ru(1)−C(2)	2.087(5)	Ru(1)−C(1)	2.01(2)
Ru(1)−C(13)	2.071(6)	O(1)−C(1)	1.02(3)
Ru(1)−O(101)	1.881(10)	O(101)−C(101)	1.37(2)
O(101)−Ru(1)−C(1)	16.2(4)	C(13)−Ru(1)−C(2)	180.000(1)
O(101)−Ru(1)−C(13)	83.4(3)	C(101)−O(101)−Ru(1)	135.2(9)
C(1)−Ru(1)−C(13)	90.8(6)	O(1)−Ru(1)−C(1)	165.4(19)
O(101)−Ru(1)−C(2)	96.6(3)	C(1)−Ru(1)−C(2)	89.2(6)

The five-membered imidazole rings of the IMes ligands in **1** are twisted 32.3° from coplanarity. This, and the fact that the two sets of opposing phenyl rings are not equally spaced, is a feature observed to varying degrees in all of the other structurally characterized bis-carbene complexes reported in this paper (see last section of Results and Discussion). The most notable feature of the structure is the *trans* geometry of the two hydrides, an unusual orientation given the strong *trans* influence of the hydride ligand. Indeed, few stable *trans*-dihydride complexes are known.[15] Similarly, while alcohol complexes of transition metals have been invoked in a number of catalytic hydrogenation reactions,[16] there are relatively few structurally characterized examples, the majority of these being cationic.[17]

Clearly the formation of **1** from $Ru(AsPh_3)(IMes)_2(CO)H_2$ does not involve a simple substitution of arsine by ethanol since an isomerization from *cis*-RuH_2 to *trans*-RuH_2 also occurs. In accord with the stereochemistry found in the solid state, the ^1H NMR spectrum of **1** in C_6D_6 showed only one single high-field hydride resonance at δ −23.51, which integrates in a ratio of 2:2:3 with two signals at δ 3.81 and 1.13 for the coordinated ethanol. The $^{13}C\{^1H\}$ NMR spectrum displayed two singlets at δ 69.7 and 23.3 for the Ru-HOEt group, while two low-field resonances at 197.9 and 205.6 ppm were assigned to the Ru-*C*(IMes) and *C*O groups, respectively. The IR spectrum of **1** contained a single ν(CO) absorption band at 1886 cm^{-1}, the low frequency presumably reflecting the presence of two strongly σ-donating IMes ligands.

Scheme 3

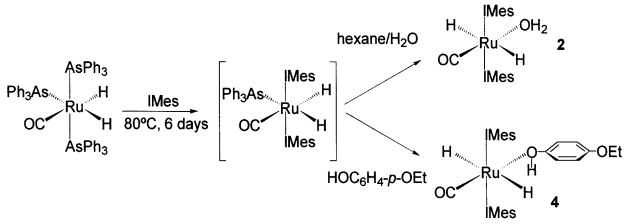

Replacement of ethanol by hexane as the crystallizing solvent afforded aqua complex $Ru(IMes)_2(CO)(H_2O)H_2$, **2**, which was isolated in 37% yield (Scheme 3). This product presumably arises due to the presence of adventitious water, but all attempts to use more rigorously dry conditions led simply to lower yields of **2**. Moreover, when degassed but undried hexane was used for crystallization, yields of **2** in excess of 80% were isolated. Crystallization with D_2O-saturated hexane gave $Ru(IMes)_2(CO)(D_2O)H_2$ (**2**-D_2O). An X-ray crystal structure determination of **2** showed the molecular geometry to be isostructural with that of **1** (Figure 2) with *trans* IMes and hydride ligands. The Ru−OH_2 distance of 2.023(2) Å (Table 2) is not unusual[20] and compares with a Ru−HOEt distance of 1.881(10) Å in **1**. No disorder was observed in the structure of **2**,

(15) (a) Shaw, B. L.; Uttley, M. F. *J. Chem. Soc., Chem. Commun.* **1974**, 918. (b) Yoshida, T.; Otsuka, S. *J. Am. Chem. Soc.* **1977**, *99*, 2134. (c) Paonessa, R. S.; Trogler, W. C. *J. Am. Chem. Soc.* **1982**, *104*, 1138. (d) Fryzuk, M. D.; MacNeil, P. A. *Organometallics* **1983**, *2*, 682. (e) Rybtchinski, B.; Ben-David, Y.; Milstein, D. *Organometallics* **1997**, *16*, 3786. (f) Li, S.; Hall, M. B. *Organometallics* **1999**, *18*, 5682.

(16) (a) Schrock, R. R.; Osborn, J. A. *J. Chem. Soc., Chem. Commun.* **1970**, 567. (b) Crabtree, R. H.; Demou, P. C.; Eden, D.; Mihelcic, J. M.; Parnell, C. A.; Quirk, J. M.; Morris, G. E. *J. Am. Chem. Soc.* **1982**, *104*, 6994. (c) Landis, C. R.; Halpern, J. *J. Am. Chem. Soc.* **1987**, *109*, 1746. (d) Persson, B. A.; Larsson, A. L. E.; Le Ray, M.; Bäckvall, J. E. *J. Am. Chem. Soc.* **1999**, *121*, 1645. (e) Laxmi, Y. R. S.; Bäckvall, J. E. *Chem. Commun.* **2000**, 611. (f) Voges, M. H.; Bullock, R. M. *J. Chem. Soc., Dalton Trans.* **2002**, 759.

(17) Neutral alcohol complexes: (a) Viñas, C.; Nuñez, R.; Teixidor, F.; Kivekäs, R.; Sillanpää, R. *Organometallics* **1996**, *15*, 3850. Cationic alcohol complexes: (b) Agbossou, S. K.; Smith, W. W.; Gladysz, J. A. *Chem. Ber.* **1990**, *123*, 1293. (c) Song, J.-S.; Szalda, D. J.; Bullock, R. M.; Lawrie, C. J. C.; Rodkin, M. A., Norton, J. R. *Angew. Chem., Int. Ed. Engl.* **1992**, *31*, 1233. (d) Milke, J.; Missling, C.; Sünkel, K.; Beck, W. *J. Organomet. Chem.* **1993**, *445*, 219. (e) Song, J.-S.; Szalda, D. J.; Bullock, R. M. *Organometallics* **2001**, *20*, 3337. (f) Dell'Amico, D. B.; Calderazzo, F.; Grazzini, A.; Labella, L.; Marchetti, F. *Inorg. Chim. Acta* **2002**, *334*, 411.

(18) (a) Cole-Hamilton, D. J.; Wilkinson, G. *Nouv. J. Chim.* **1977**, *1*, 141. (b) Bruno, J. W.; Huffmann, J. C.; Caulton, K. G. *Inorg. Chim. Acta* **1984**, *89*, 167. (c) Van Der Sluys, L. S.; Kubas, G. J.; Caulton, K. G. *Organometallics* **1991**, *10*, 1033. (d) Chen, Y.-Z.; Chan, W. C.; Lau, C. P.; Chu, H. S.; Lee, H. L.; Jia, G. *Organometallics* **1997**, *16*, 1241.

(19) The IR bands of **3** are moved to lower frequency than those in the related complex *trans*,*cis*,*cis*-$Ru(PMe_3)_2(CO)_2H_2$ containing strongly electron-donating trimethylphosphine ligands. Mawby, R. J.; Perutz, R. N.; Whittlesey, M. K. *Organometallics* **1995**, *14*, 3268.

(20) (a) Boniface, S. M.; Clark, G. R.; Collins, T. J.; Roper, W. R. *J. Organomet. Chem.* **1981**, *206*, 109. (b) Sun, Y.; Taylor, N. J.; Carty, A. J. *Inorg. Chem.* **1993**, *32*, 4457.

Table 2. Selected Bond Lengths [Å] and Angles [deg] for $Ru(IMes)_2(CO)(H_2O)H_2$ (2)

Ru(1)−C(43)	1.798(3)	Ru(1)−O(2)	2.023(2)
Ru(1)−C(22)	2.066(2)	Ru(1)−C(1)	2.069(2)
O(1)−C(43)	1.165(3)		
C(43)−Ru(1)−O(2)	174.90(13)	C(43)−Ru(1)−C(22)	91.25(11)
O(2)−Ru(1)−C(22)	88.19(9)	C(43)−Ru(1)−C(1)	93.23(11)
O(2)−Ru(1)−C(1)	87.43(9)	C(22)−Ru(1)−C(1)	175.43(9)

although the hydrogen atoms on the bound water could not be reliably located.

The spectroscopic features of **2** are similar to those of the ethanol complex. In the ^{1}H NMR spectrum, the hydride resonance for **2** is shifted only 0.36 ppm downfield relative to **1**. The carbonyl absorption bands come at moderately different frequencies (**1**, 1886 cm^{-1}; **2**, 1861 cm^{-1}). The ^{1}H NMR spectrum of **2** showed a broad resonance as a consequence of the coordinated water at δ 0.93. This signal remained broad even upon cooling to −80 °C, but disappeared upon shaking with D_2O.

Thermolytic Stability of 1 and 2. Thermolysis of **1** in C_6D_6 at 90 °C for 2 weeks yielded the bis-carbene dihydride complex $Ru(IMes)_2(CO)_2H_2$ (**3**) resulting from decarbonylation of the coordinated ethanol (eq 2).[18] The

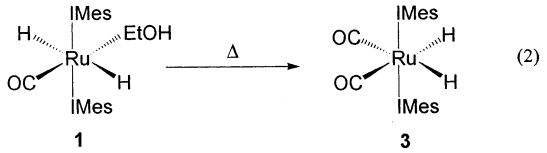

(2)

1 **3**

^{1}H NMR spectrum of **3** contained a single hydride resonance at δ −6.53, shifted significantly downfield relative to that seen for **1**. The appearance of only one Ru-*C*O resonance (204.3 ppm) in the $^{13}C\{^1H\}$ NMR spectrum and two ν_{CO} bands in the IR spectrum (1973, 1936 cm^{-1}) indicate that **3** possesses a *tcc*-stereochemistry.[19] In contrast to **1**, the aqua complex is thermally stable even at 100 °C, as evidenced by the lack of detectable change in the ^{1}H NMR spectrum at that temperature over 3 days.

Reaction of 1 and 2 with O-Donor Ligands. The ^{1}H NMR spectrum of **1** in C_6D_6 recorded following addition of a 20-fold excess of water showed significant broadening of the hydride signal at δ −23.51 (the resonances for the coordinated ethanol ligand were unaffected), but no resonance for the aqua complex **2** was detected. Hydride signal broadening was also observed upon addition of EtOH to solutions of the aqua complex. These observations suggest either the presence of intermolecular M−H···H−OR hydrogen bonding interactions, examples of which have recently been reported,[21] or Ru−H/H−OR exchange (see below).

No reaction was seen upon addition of DMSO, THF, or pyridine to benzene solutions of **1** or **2**. Expecting that donor ligand bulk was responsible for this lack of reaction, we were somewhat surprised to find that the phenol HOC_6H_4-*p*-OEt displaced the water in **2** (Scheme 3) to give $Ru(IMes)_2(CO)(HOC_6H_4$-*p*-$OEt)H_2$ (**4**), which exhibited spectroscopic properties similar to that of the parent aqua complex (^{1}H, δ −24.48; IR, ν(CO) 1881 cm^{-1}). Although single crystals of **4** were obtained by direct reaction of $Ru(IMes)_2(AsPh_3)(CO)H_2$ with the phenol, they were of insufficient quality to facilitate a good structural analysis by X-ray crystallography. However, the solid state structure served to confirm at least that the ruthenium was bonded to the phenolic oxygen rather than the oxygen of the ethoxy substituent.

Scheme 4

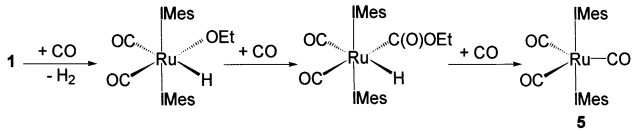

5

Reaction of 1 and 2 with CO. Addition of CO to a solution of complex **1** at room temperature resulted in an immediate color change from yellow to clear and then back to orange-yellow, affording the ruthenium(0) complex $Ru(IMes)_2(CO)_3$ (**5**) over the course of a day. The spectroscopic features of **5** are consistent with a trigonal bipyramidal structure where the three CO ligands are located in the equatorial plane.[22] Thus, the proton NMR spectrum showed just two sets of methyl resonances integrating in a ratio of 2:1 for the *ortho*- and *para*-mesityl groups of the IMes ligands. The $^{13}C\{^1H\}$ NMR spectrum displayed one very low-field carbonyl resonance (217.6 ppm), while three ν_{CO} absorption bands appeared in the IR spectrum recorded in KBr at 1950, 1879, and 1830 cm^{-1}. The tricarbonyl complex was also identified as the final product upon addition of CO to solutions of the aqua complex **2**, although in this case, 5 days were required for reaction completion at room temperature (see below).

Mechanism of Reaction of 1 with CO. The ultimate formation of $Ru(IMes)_2(CO)_3$ from addition of CO to solutions of **1** or **2** implies a similar reaction pathway in both cases, although the different completion times suggest different stabilities and reactivity of intermediate species along the way. This was investigated in more detail by labeling experiments with ^{13}CO. The ^{1}H NMR spectrum recorded within 1 h of addition of ^{13}CO to a C_6D_6 solution of **1** showed the complete disappearance of starting material and formation of two new hydride products with resonances at δ −3.86 (d, J_{HC} = 43.7 Hz) and −5.22 (dd, J_{HC} = 33.5, J_{HC} = 5.4 Hz), which were assigned as $Ru(IMes)_2(CO)_2(OEt)H$ and the CO insertion product $Ru(IMes)_2(CO)_2(C(O)OEt)H$,[23] respectively (Scheme 4). The 30−45 Hz ^{1}H−^{13}C coupling constant seen for both species is consistent with ^{13}CO incorporation *trans* to Ru−H, while the small J value seen on the CO insertion product is due to coupling to the Ru-^{13}C(O)OEt ligand. Additionally, the ^{1}H NMR spectrum

(21) (a) Shubina, E. S.; Belkova, N. V.; Krylov, A. N.; Vorontsov, E. V.; Epstein, L. M.; Gusev, D. G.; Niedermann, M.; Berke, H. *J. Am. Chem. Soc.* **1996**, *118*, 1105. (b) Guari, Y.; Ayllon, J. A.; Sabo-Etienne, S.; Chaudret, B. *Inorg. Chem.* **1998**, *37*, 640. (c) Messmer, A.; Jacobsen, H.; Berke, H. *Chem. Eur. J.* **1999**, *5*, 3341.

(22) Rossi, A. R.; Hoffmann, R. *Inorg. Chem.* **1975**, *14*, 365.

(23) Reaction of M−OR with CO can lead to a range of products depending on the other ancillary ligands on the metal. CO insertion into M−OR: (a) Bennett, M. A.; Robertson, G. B.; Whimp, P. O.; Yoshida, T. A. *J. Am. Chem. Soc.* **1973**, *95*, 3028. (b) Bennett, M. A.; Yoshida, T. A. *J. Am. Chem. Soc.* **1978**, *100*, 1750. (c) Michelin, R. A.; Napoli, M.; Ros, R. *J. Organomet. Chem.* **1979**, *175*, 239. (d) Bryndza, H. E.; Kretchmar, S. A.; Tulip, T. H. *J. Chem. Soc., Chem. Commun.* **1985**, 977. (e) Bryndza, H. E. *Organometallics* **1985**, *4*, 1686. (f) Kim, Y.-J.; Osakabd, K.; Sugita, K.; Yamamoto, T.; Yamamoto, A. *Organometallics* **1988**, *7*, 2182. Insertion of CO into M−C rather than M−OR: Hartwig, J. F.; Bergman, R. G.; Andersen, R. A. *J. Am. Chem. Soc.* **1991**, *113*, 6499. CO-induced reductive elimination: Glueck, D. S.; Newman Winslow, L. J.; Bergman, R. G. *Organometallics* **1991**, *10*, 1462.

displayed two sets of ethoxide signals at 3.69 and 1.44 ppm (J_{HH} = 6.6 Hz) for the ethoxy hydride and 4.12 and 1.23 ppm (J_{HH} = 7.0 Hz) for the ethoxycarbonyl hydride. A single ^{13}C-enhanced CO resonance at δ 195.2 was observed for Ru(IMes)$_2$(CO)$_2$(OEt)H by ^{13}C{^{1}H} NMR spectroscopy, while two ^{13}C-enriched doublet signals at δ 202.9 (J_{CC} = 4.5 Hz) and 198.5 (J_{CC} = 4.5 Hz) for Ru(IMes)$_2$(CO)$_2$(C(O)OEt)H are in agreement with the presence of coupled Ru-^{13}CO and Ru-^{13}C(O)OEt groups.[24]

After 4 h at room temperature, NMR showed complete conversion of Ru(IMes)$_2$(CO)$_2$(OEt)H to Ru(IMes)$_2$(CO)$_2$(C(O)OEt)H; a small amount of **5** was apparent in the ^{13}C{^{1}H} NMR spectrum. Over longer time, ^{13}C{^{1}H} NMR spectroscopy simply shows depletion of Ru(IMes)$_2$(CO)$_2$(C(O)OEt)H (a small amount of all ^{13}CO-labeled Ru(IMes)$_2$(^{13}CO)$_2$(^{13}C(O)OEt)H is produced) and an increase in the amount **5**. We see no other species (including free CO_2) during this conversion.

Reaction of CO with 2. In an analogous manner to the reaction seen between CO and **1**, addition of 1 atm of CO to a C_6D_6 solution of **2** resulted in an instantaneous color change from yellow to colorless. The ^{1}H NMR spectrum of the colorless solution showed the presence of the hydroxy hydride complex Ru(IMes)$_2$(CO)$_2$(OH)H (**6**) as the major species, along with a much smaller concentration of Ru(IMes)$_2$(CO)$_3$ (**5**). The hydroxy hydride complex displayed a single hydride resonance moved significantly to lower field (δ −4.27) relative to that for **1**, consistent with a CO ligand *trans* to hydride rather than a *trans* H−Ru−H stereochemistry; this shift to lower field is observed in all cases where a *cis*-Ru(CO)$_2$(X)H unit is formed in reactions with CO.[25] The ^{1}H NMR spectrum of **6** also showed a broad hydroxyl resonance (δ −3.75) which sharpened upon cooling to −70 °C.[6,26] The chemical shift of the hydroxyl proton in **6** is comparable to those reported for other late metal 18-electron hydroxy complexes, including *trans*-Ru(dmpe)$_2$(OH)H,[27] *cis*-Ru(PMe$_3$)$_4$(OH)H,[27] *cis*-Ru(PMe$_3$)$_4$(OH)(Ph),[28] and *cis*-[Ir(PMe$_3$)$_4$(OH)H]$^+$,[29] which appear at −4.55, −3.79, −4.47, and −1.40 ppm, respectively. When the formation of **6** was repeated using ^{13}CO, the hydride signal displayed an additional doublet splitting of 43.6 Hz, the magnitude of this coupling being consistent with ^{13}CO incorporation exclusively *trans* to hydride.

X-ray Crystal Structure of Ru(IMes)$_2$(CO)$_2$(OH)H (6). Due to the paucity of structurally characterized hydroxy hydride complexes,[28,30] the molecular structure of Ru(IMes)$_2$(CO)$_2$(OH)H was confirmed by a single-crystal X-ray structure determination as shown in Figure 3. Selected bond distances and angles are given in Table 3. The complex has distorted octahedral geometry with a strained *trans* arrangement of both the IMes ligands (C(3)−Ru−C(24) = 167.94(8)°) and the hydroxo group *trans* to the carbonyl (C(2)−Ru−O(3) = 172.7(4)°). The Ru−O distance of 2.058(3) Å is significantly shorter than that seen in [*trans*-Ru(dmpe)$_2$(OH)H·H$_2$O]$_2$ (2.230(2) Å), presumably due to the larger *trans* influence of H compared to CO.[27a] The weaker *trans* influence of OH relative to hydride explains the two quite different Ru−CO distances found in the structure of **6** (1.966(3), 1.873(6) Å).

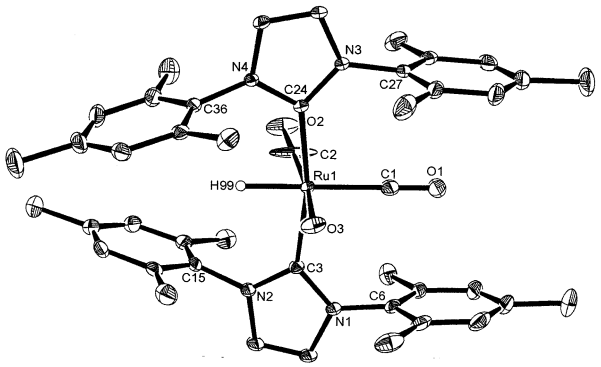

Figure 3. ORTEX diagram of Ru(IMes)$_2$(CO)$_2$(OH)H (**6**). Thermal ellipsoids are shown at the 30% probability level.

Table 3. Selected Bond Lengths [Å] and Angles [deg] for Ru(IMes)$_2$(CO)$_2$(OH)H (6)

Ru(1)−C(2A)	1.931(14)	Ru(1)−C(2)	1.873(6)
Ru(1)−O(3)	2.058(3)	Ru(1)−C(1)	1.966(3)
Ru(1)−C(24)	2.101(2)	Ru(1)−O(3A)	2.10(2)
O(1)−C(1)	1.144(3)	Ru(1)−C(3)	2.113(2)
		O(2)−C(2)	1.207(7)
C(2)−Ru(1)−C(2A)	150.5(6)	C(2A)−Ru(1)−C(1)	111.9(5)
C(2)−Ru(1)-C(1)	97.5(4)	C(2)−Ru(1)-O(3)	172.7(4)
C(2A)-Ru(1)−O(3)	22.8(4)	C(1)−Ru(1)-O(3)	89.44(15)
C(2A)-Ru(1)−O(3A)	154.5(6)	C(2)−Ru(1)-O(3A)	4.4(6)
O(3)−Ru(1)-O(3A)	174.9(4)	C(1)−Ru(1)-O(3A)	93.6(3)
C(2)−Ru(1)-C(24)	88.7(2)	C(2A)-Ru(1)−C(24)	90.1(3)
C(1)−Ru(1)-C(24)	96.22(9)	O(3)−Ru(1)-C(24)	88.49(10)
O(3A)-Ru(1)−C(24)	87.1(4)	C(2A)-Ru(1)−C(3)	82.5(3)
C(2)−Ru(1)-C(3)	93.1(2)	O(3)−Ru(1)-C(3)	88.28(11)
C(1)−Ru(1)-C(3)	95.37(9)	C(24)−Ru(1)-C(3)	167.94(8)
O(3A)-Ru(1)−C(3)	95.5(4)		

Formation of Ru(IMes)$_2$(CO)$_3$ from 2. The slower conversion of **2** to **5** compared to the formation of **5** from the ethanol complex **1** prompted us to probe the mechanism of the reaction by ^{13}CO labeling in an attempt to identify any intermediates. Thus, addition of ^{13}CO to **2** showed by ^{13}C{^{1}H} NMR the hydroxy hydride complex **6** and a small amount of **5**. Over time, as **6** was depleted and **5** grows in, we also detected an additional, minor product, which was identified as the η^1-bicarbonate complex Ru(IMes)$_2$(CO)$_2$(OC(O)OH)H (**7**), on the basis of an alternative synthetic route as reported below. We postulate that **5**, **6**, and **7** are formed via the mechanism shown in Scheme 5. The hydroxy hydride inserts CO[31] in an analogous way to Ru(IMes)$_2$(CO)$_2$(OEt)H, but the resulting Ru(IMes)$_2$(CO)$_2$(C(O)OH)H species readily de-

(24) Holland, P. L.; Andersen, R. A.; Bergman, R. G. *J. Am. Chem. Soc.* **1996**, *118*, 1092.

(25) (a) Heyn, R. H.; Macgregor, S. A.; Nadasdi, T. T.; Ogasawara, M.; Eisenstein, O.; Caulton, K. G. *Inorg. Chim. Acta* **1997**, *259*, 5. (b) Cooper, A. C.; Bollinger, J. C.; Huffman, J. C.; Caulton, K. G. *New J. Chem.* **1998**, *22*, 473.

(26) Edwards, A. J.; Elipe, S.; Esteruelas, M. A.; Lahoz, F. J.; Oro, L. A.; Velero, C. *Organometallics* **1997**, *16*, 3828.

(27) (a) Burn, M. J.; Fickes, M. G.; Hartwig, J. F.; Hollander, F. J.; Bergman, R. G. *J. Am. Chem. Soc.* **1993**, *115*, 5875. (b) Kaplan, A. W.; Bergman, R. G. *Organometallics* **1997**, *16*, 1106.

(28) Hartwig, J. F.; Bergman, R. G.; Andersen, R. A. *J. Am. Chem. Soc.* **1991**, *113*, 3404.

(29) Milstein, D.; Calabrese, J. C.; Williams, I. D. *J. Am. Chem. Soc.* **1986**, *108*, 6387.

(30) (a) Stevens, R. C.; Bau, R.; Milstein, D.; Blum, O.; Koetzle, T. F. *J. Chem. Soc., Dalton Trans.* **1990**, 1429. (b) Dorta, R.; Togni, A. *Organometallics* **1998**, *17*, 3423. (c) Renkema, K. B.; Huffman, J. C.; Caulton, K. G. *Polyhedron* **1999**, *18*, 2575. (d) Morales-Morales, D.; Lee, D. W.; Wang, Z.; Jensen, C. M. *Organometallics* **2001**, *20*, 1144. (e) Dorta, R.; Rosenberg, H.; Shimon, L. J. W.; Milstein, D. *J. Am. Chem. Soc.* **2002**, *124*, 188. (f) Blum, O.; Milstein, D. *J. Am. Chem. Soc.* **2002**, *124*, 11456.

(31) Addition of ^{13}CO to Ru(IMes)$_2$(CO)$_2$(OH)H leads to ^{13}CO incorporation into the hydroxy hydride, *trans* to the hydride.

Scheme 5

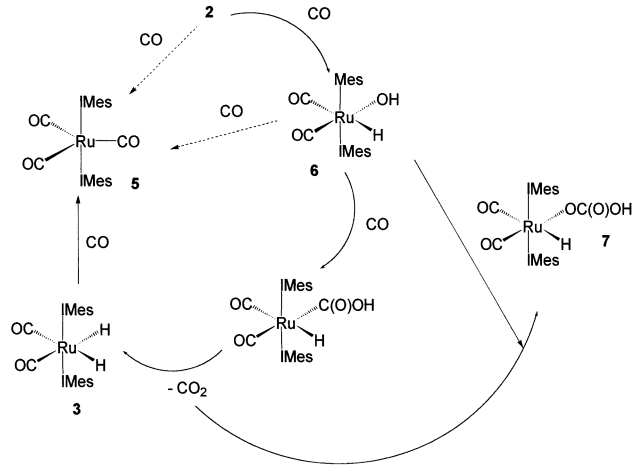

Scheme 6

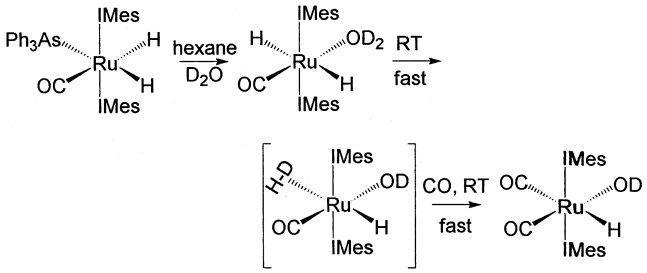

carboxylates to give **3** and CO_2. The dihydride complex **3** then reacts with CO to afford **5**, while CO_2 inserts into the Ru−OH bond of $Ru(IMes)_2(CO)_2(OH)H$ to yield the bicarbonate complex **7**. When an isolated sample of the hydroxy hydride complex was reacted with CO_2, **7** was indeed formed as the only product, giving strong support to this step of the proposed scheme. The initial formation of some $Ru(IMes)_2(CO)_3$ upon addition of CO to **2** implies that there must be a minor pathway to the tricarbonyl either directly from the water complex or via the hydroxy hydride.

Formation of $Ru(IMes)_2(CO)_2(OH)H$ from $Ru(IMes)_2(CO)(H_2O)H_2$. The pathway to formation of $Ru(IMes)_2(CO)_2(OH)H$ was probed by deuterium labeling studies. The ^1H NMR spectrum recorded after addition of CO to a C_6D_6 solution of $Ru(IMes)_2(CO)(D_2O)H_2$ (**2**-D_2O) displayed the expected hydride resonance at δ −4.27, but showed no OH peak, indicating the formation of $Ru(IMes)_2(CO)_2(OD)H$. This observation, together with the exclusive ^{13}CO incorporation *trans* to hydride described above, is consistent with formation of the hydroxy hydride via proton transfer rather than oxidative addition of water (Scheme 6).[27a,30b,e,32]

Hence, we propose that protonation of one of the strongly hydridic hydride ligands by the (acidic) coordinated water yields a putative dihydrogen hydroxy hydride species, which readily dissociates H_2 in the presence of CO.[33] Additional evidence for this protonation pathway was revealed upon treatment of a C_6D_6 solution of **2** with a slight excess of D_2O. The intensity of the hydride signal readily depleted, as evidenced by the relative integrations of Ru−H:aryl:methyl signals

(32) Tani, K.; Iseki, A.; Yamagata, T. *Angew. Chem., Int. Ed.* **1998**, *37*, 3381.

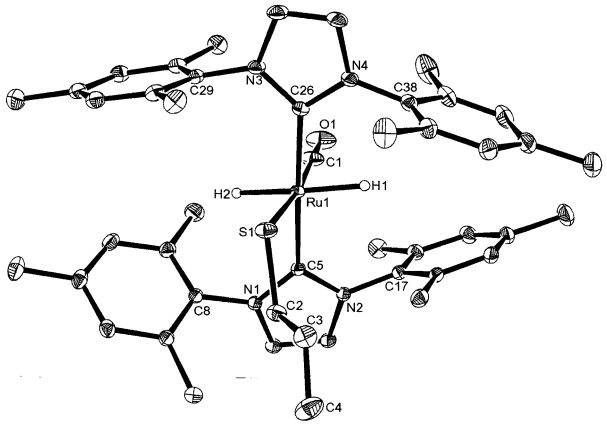

Figure 4. ORTEX diagram of $Ru(IMes)_2(CO)(HSCH_2CH_2CH_3)H$ (**8**). Thermal ellipsoids are shown at the 30% probability level.

Scheme 7

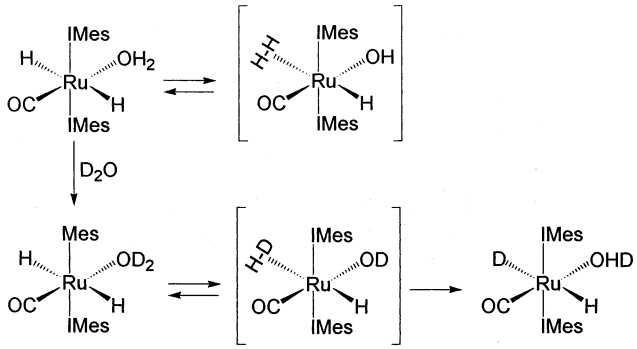

(1:18:81 rather than the expected 1:4:18 recorded after 5 days at 50 °C), indicating Ru−H/D_2O exchange. After 3 weeks at 75 °C, ^1H NMR spectroscopy showed only traces of the hydride signal remaining. The pathway for this exchange process is shown in Scheme 7, proceeding by the same dihydrogen (or hydrogen−deuterium) hydroxy hydride species.[34]

Reaction of 1 and 2 with Propanethiol. Propanethiol ($CH_3CH_2CH_2SH$) readily substituted the coordinated solvent ligands in both **1** and **2** to afford the same thiol dihydride product $Ru(IMes)_2(CO)(HSCH_2CH_2CH_3)H_2$ (**8**). While we were unable to observe the S−H resonance in the ^1H NMR spectrum of **8**, the appearance of a single high-field hydride resonance (δ −23.77), similar to that seen for **1**, **2**, and **4**, implies the presence of a two-electron RSH ligand *trans* to CO. The X-ray crystal structure of **8** is shown in the ORTEX plot in Figure 4. Table 4 contains relevant bond angles and distances. The geometry at ruthenium is very close to octahedral with a *trans*-C(5)−Ru−C(26)

(33) (a) Crabtree, R. H.; Lavin, M.; Bonneviot, L. *J. Am. Chem. Soc.* **1986**, *108*, 4032. (b) Jensen, C. M.; Trogler, W. C. *J. Am. Chem. Soc.* **1986**, *108*, 723. (c) Leoni, P.; Sommovigo, M.; Pasquali, M.; Midollini, S.; Braga, D.; Sabatino, P. *Organometallics* **1991**, *10*, 1038. (d) Kubas, G. J.; Burns, C. J.; Khalsa, G. R. K.; Van Der Sluys, L. S.; Kiss, G.; Hoff, C. D. *Organometallics* **1992**, *11*, 3390. (e) Milet, A.; Dedieu, A.; Kapteijn, G.; van Koten, G. *Inorg. Chem.* **1997**, *36*, 3223.

(34) Proton NMR spectra recorded over the course of the reaction between **2** and D_2O also showed a smaller than expected integral for the NCH=CHN backbone protons of the IMes ligands, raising the likelihood of H/D exchange here also. H/D exchange into the backbone positions using D_2O has been reported in the free carbene ligand. (a) Denk, M. K.; Rodezno, J. M. *J. Organomet. Chem.* **2000**, *608*, 122. (b) Denk, M. K.; Rodezno, J. M. *J. Organomet. Chem.* **2001**, *617*−*618*, 737.

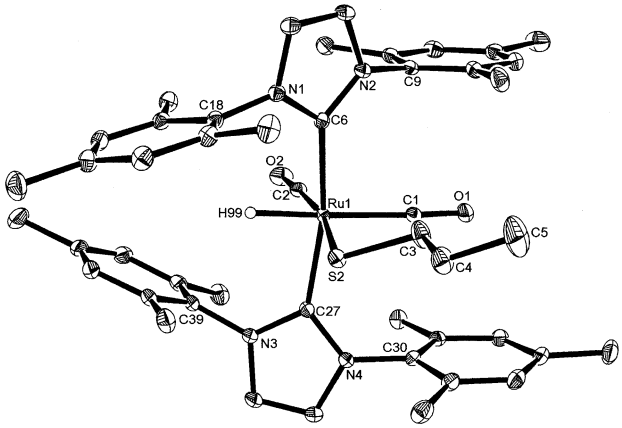

Figure 5. ORTEX diagram of $Ru(IMes)_2(CO)_2(SCH_2CH_2CH_3)H$ (**9**). Thermal ellipsoids are shown at the 30% probability level.

Table 4. Selected Bond Lengths [Å] and Angles [deg] for $Ru(IMes)_2(CO)(HSCH_2CH_2CH_3)H_2$ (8)

Ru(1)−C(1)	1.8258(14)	Ru(1)−C(5)	2.0874(11)
Ru(1)−C(26)	2.0917(11)	Ru(1)−S(1)	2.3706(15)
Ru(1)−S(1A)	2.425(3)	S(1)−C(2)	1.8401(19)
O(1)−C(1)	1.1578(18)		
C(1)−Ru(1)−C(5)	87.91(5)	C(1)−Ru(1)−C(26)	90.32(5)
C(5)−Ru(1)−C(26)	177.56(4)	C(1)−Ru(1)−S(1)	173.27(6)
C(5)−Ru(1)−S(1)	95.23(5)	C(26)−Ru(1)−S(1)	86.71(5)
C(1)−Ru(1)−S(1A)	173.67(8)	C(5)−Ru(1)−S(1A)	96.11(8)
C(26)−Ru(1)−S(1A)	85.51(8)	S(1)−Ru(1)−S(1A)	10.85(6)
C(2)−S(1)−Ru(1)	114.80(8)		

Scheme 8

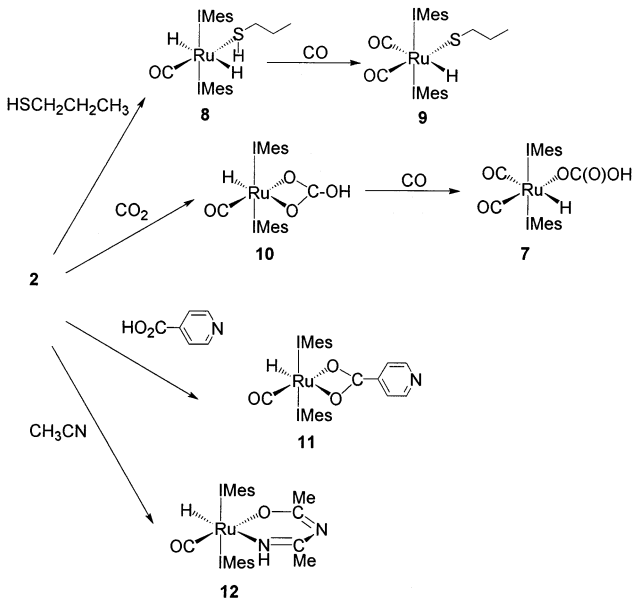

angle of 177.56(4)°. Disorder in the sulfur position (68:32) precluded reliable location of the SH hydrogen. The occupancy ratio of the sulfur implies that the Ru−S bond length is closer to the value of 2.3706(15) Å found for Ru−S(1); this distance is in line with other Ru(II) thiol complexes.[35]

The thiolate hydride complex $Ru(IMes)_2(CO)_2(SCH_2CH_2CH_3)H$ (**9**) was formed in good yield upon treatment of **8** with CO (Scheme 8). The hydride signal for **9** was observed in the ^1H NMR spectrum at δ −4.10, while the resonances for the propyl chain (2.16, 1.89, and 1.20 ppm) were assigned on the basis of COSY spectroscopy. The IR spectrum shows three strong bands between 2015 and 1890 cm^{-1}, with that at 1946 cm^{-1} (enhanced due to intensity stealing) assigned to ν_{Ru-H} on the grounds of the observed shift to lower frequency of the other two bands upon ^{13}CO labeling.

Table 5. Selected Bond Lengths [Å] and Angles [deg] for $Ru(IMes)_2(CO)_2(SCH_2CH_2CH_3)H$ (9)

Ru(1)−C(1)	1.9546(18)	Ru(1)−C(2)	1.8629(17)
Ru(1)−C(6)	2.1207(16)	Ru(1)−C(27)	2.1086(16)
Ru(1)−S(2)	2.4539(4)	O(1)−C(1)	1.142(2)
O(2)−C(2)	1.149(2)		
C(2)−Ru(1)−C(1)	97.81(7)	C(1)−Ru(1)−C(27)	97.69(7)
C(2)−Ru(1)−C(27)	91.43(7)	C(2)−Ru(1)−C(6)	94.04(7)
C(1)−Ru(1)−C(6)	94.41(6)	C(27)−Ru(1)−C(6)	165.91(6)
C(1)−Ru(1)−S(2)	92.94(5)	C(2)−Ru(1)−S(2)	168.89(6)
C(6)−Ru(1)−S(2)	87.87(4)	C(27)−Ru(1)−S(2)	84.35(5)
O(1)−C(1)−Ru(1)	177.57(15)	C(3)−S(2)−Ru(1)	106.75(7)
		O(2)−C(2)−Ru(1)	176.62(16)

The structure of **9** was confirmed by X-ray diffraction, as shown in Figure 5. Selected bond distances and angles for **9** are given in Table 5. As in the structure of the hydroxy hydride **6**, the coordination geometry around the central ruthenium in **9** is distorted from a regular octahedron with highly bent *trans*-IMes−Ru−IMes and *cis*-$Ru(CO)_2$ angles (C(6)−Ru−C(27) 165.91(6)°, C(2)−Ru−C(1) 97.81(7)°). The two Ru−CO bond lengths exhibit significant differences (1.9546(18), 1.8629(17) Å), while the Ru−S distance at 2.4539(4) Å is comparable to that reported for other Ru(II) thiolate complexes.[36] The high acidity of coordinated thiol ligands[37] combined with the instability of many thiol complexes[38] helps to explain the paucity of structurally characterized thiol complexes. The transformation of **8** into **9** upon reaction with CO is presumed to follow a protonation or hydrogen transfer pathway similar to that described above for formation of $Ru(IMes)_2(CO)_2(OH)H$. Support for such a process comes from the work of James and co-workers, who have reported H/D exchange of both Ru−SH and Ru−H in $Ru(PPh_3)_2(CO)_2(SH)H$ in C_6D_6 solution containing traces of CD_3OD.[36d]

Reaction of 2 with CO_2. Addition of 1 atm of dry CO_2 to a C_6D_6 solution of **2** resulted in an immediate color change from yellow to colorless and precipitation of a white solid, which analyzed as the bidentate bicarbonate complex $Ru(IMes)_2(CO)(\kappa^2\text{-}O_2COH)H$, **10** (Scheme 8). The ^1H NMR spectrum showed a hydride resonance for **10** at δ −20.73 and a broad OH signal for the bicarbonate at δ 8.80; the bicarbonate carbon atom appeared as a distinctive singlet at 160.3 ppm in the

(35) Amarasekera, J.; Rauchfuss, T. B. *Inorg. Chem.* **1989**, *28*, 3875.

(36) (a) Mura, P.; Olby, B. G.; Robinson, S. D. *J. Chem. Soc., Dalton Trans.* **1985**, 2101. (b) Mura, P.; Olby, B. G.; Robinson, S. D. *Inorg. Chim. Acta*, **1985**, *98*, L21. (c) Jessop, P. G.; Rettig, S. J.; Lee, C.-L.; James, B. R. *Inorg. Chem.* **1991**, *30*, 4617. (d) Jessop, P. G.; Lee, C.-L.; Rastar. G. James, B. R., Lock, C. J. L.; Faggiani, R. *Inorg. Chem.* **1992**, *31*, 4601. (e) Field, L. D.; Hambley, T. W.; Yau, B. C. K. *Inorg. Chem.* **1994**, *33*, 2009. (f) Coto, A.; de los Ríos, I.; Jiménez Tenorio, M.; Puerta, M. C.; Valerga, P. *J. Chem. Soc., Dalton Trans.* **1999**, 4309.

(37) (a) Treichel, P. M.; Rosenhein, L. D. *Inorg. Chem.* **1981**, *20*, 942. (b) Urban G.; Sunkel, K.; Beck, W. *J. Organomet. Chem.* **1985**, *290*, 329. (c) Treichel, P. M.; Schmidt, M. S.; Crane, R. A. *Inorg. Chem.* **1991**, *30*, 379. (d) Deeming, A. J.; Doherty, S.; Marshall, J. E.; Powell, J. L.; Senior, A. M. *J. Chem. Soc., Dalton Trans.* **1993**, 1093.

(38) Peruzzini, M.; de los Ríos, I.; Romerosa, A. *Prog. Inorg. Chem.* **2001**, *49*, 169.

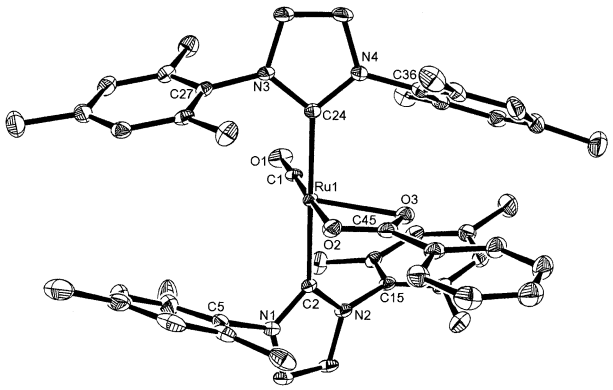

Figure 6. ORTEX diagram of $Ru(IMes)_2(CO)(\eta^2\text{-}O_2CC_5H_4N)H$ (**11**). Thermal ellipsoids are shown at the 30% probability level.

Table 6. Selected Bond Lengths [Å] and Angles [deg] for $Ru(IMes)_2(CO)(\kappa^2\text{-}O_2CC_5H_4N)H$ (11)

Ru(1)−C(1A)	1.733(6)	Ru(1)−C(1)	1.803(3)
Ru(1)−C(2)	2.0897(18)	Ru(1)−C(24)	2.0962(18)
Ru(1)−O(2)	2.2763(16)	Ru(1)−O(3)	2.2921(14)
O(1)−C(1)	1.172(4)	O(2)−C(45)	1.264(3)
O(3)−C(45)	1.257(3)		

C(1A)−Ru(1)−C(1)	56.7(3)	C(1A)−Ru(1)−C(2)	92.08(19)
C(1)−Ru(1)−C(2)	86.30(11)	C(1A)−Ru(1)−C(24)	87.76(19)
C(1)−Ru(1)−C(24)	92.63(11)	C(2)−Ru(1)−C(24)	178.82(8)
C(1A)−Ru(1)−O(2)	122.8(3)	C(1)−Ru(1)−O(2)	177.09(10)
C(2)−Ru(1)-O(2)	90.87(6)	C(24)−Ru(1)-O(2)	90.20(6)
C(1A)-Ru(1)−O(3)	175.26(18)	C(1)−Ru(1)-O(3)	123.12(12)
C(2)−Ru(1)-O(3)	92.63(6)	C(24)−Ru(1)-O(3)	87.53(6)
O(2)−Ru(1)-O(3)	57.67(6)	C(45)−O(2)-Ru(1)	90.48(14)
C(45)−O(3)-Ru(1)	89.94(13)		

$^{13}C\{^1H\}$ NMR spectrum.[39] All attempts to produce crystals of **10** suitable for X-ray crystallography proved unsuccessful. Thus, we utilized isonicotinic acid ($NC_5H_4\text{-}CO_2H$) to afford the structurally related bidentate isonicotinate complex $Ru(IMes)_2(CO)(\kappa^2\text{-}O_2CC_5H_4N)H$, **11**. The κ^2-coordination mode in both these compounds is revealed by the IR spectra, which contain symmetric OCO stretching bands at 1593 and 1596 cm^{-1} and absorption bands for the asymmetric stretching modes at 1453 and 1461 cm^{-1}, respectively.[40,41]

The κ^2-coordination mode in **11** was authenticated by an X-ray crystal structure determination (Figure 6). Selected geometric data are given in Table 6. The $\kappa^2\text{-}O_2CC_5H_4N$ ligand sits almost perfectly perpendicular to the IMes−Ru−IMes axis with the pyridyl ring twisted 7.8° out of the RuOCO plane. The Ru−O bond lengths (2.2763(16), 2.2921(14) Å) are long in comparison to the Ru−O distances in the ruthenium carboxylate complexes $Ru(PPh_3)_2(CO)(MeOH)(OC(O)CF_3)_2$ (2.139(6), 2.101(7) Å)[42] and $Ru(PPh_3)_2(CO)_2(OC(O)Ph)_2$ (2.086(5), 2.083(7) Å)[43] or the carbonate complex $Ru(PPh_3)_2(CO)_2(O_2CO)$ (2.079(2) Å).[44]

The monodentate bicarbonate complex $Ru(IMes)_2(CO)_2(\eta^1\text{-}OC(O)OH)H$ (**7**), which was reported above as being formed as a minor product in the reaction of $Ru(IMes)_2(CO)_2(OH)H$ with CO, was isolated in nearly quantitative yield when CO was introduced into a C_6D_6 solution of **10** (Scheme 8). An alternative route to **7** involved reaction of the hydroxy hydride complex **6** with CO_2. The NMR spectra of **7** showed characteristic features for this type of ligand binding, specifically a broad low-field OH resonance in the ^1H NMR spectrum at δ 12.10 and a bicarbonate carbon signal at 162.8 ppm in the $^{13}C\{^1H\}$ NMR spectrum. The mode of bonding is also revealed by the appearance of the symmetric and asymmetric OCO stretching bands at 1605 and 1355 cm^{-1} in the IR spectrum.[26,40]

The X-ray crystal structure of **7** (Figure 7) and selected bond lengths and angles are given in Table 7. The most significant feature of this structure is the molecular packing, which demonstrates dimerization of two molecules in the asymmetric unit via hydrogen bonding of the bicarbonate groups.[45] The Ru−O distances are 2.1344(18) and 2.1352(19) Å, while the Ru−CO bond lengths are significantly different due to the different *trans* influences of −OC(O)OH and hydride. As in the other structurally characterized $Ru(IMes)_2(CO)_2(X)H$ complexes reported here, the *trans*-IMes ligands are somewhat strained (C(25)−Ru(1)−C(4) 166.85(12)°, C(125)−Ru(2)−C(4) 167.66(12)°).

Treatment of 2 with Acetonitrile: Synthesis and Characterization of an *N*-Imidoylimidato Complex. Addition of 4 equiv of acetonitrile to a C_6D_6 solution of **2** gave the *N*-imidoylimidato complex **12**, resulting from the coupling of two CH_3CN ligands in a head-to-tail manner with the Ru−OH_2 group (Scheme 8). The proton NMR spectrum of **12** shows two inequivalent metallacyclic methyl resonances (1.99, 1.52 ppm) and a singlet hydride resonance at δ −11.40. A broad feature at δ 5.73 was assigned to the N−H group. $^1H-^{13}C$ HMQC and HMBC experiments were used to assign two signals at 173.8 and 166.0 in the $^{13}C\{^1H\}$ NMR spectrum to the nitrile carbons.

A single crystal of **12** suitable for X-ray diffraction was obtained from a toluene/hexane solution. An ORTEX plot of the asymmetric unit is shown in Figure 8, while selected bond lengths and angles are given in Table 8. The *N*-imidoylimidato chelate ring is approximately flat, but not entirely planar. The maximum deviation from the least squares plane containing atoms Ru1, N5, C2, N6, and C4 is 0.08 Å (for C4), while the perpendicular distance from O2 to this plane is 0.28 Å. In this respect, the structure of **12** is a little different from the structure of $Ru(PPh_3)_2(CO)(NH{=}CRN{=}CRO)Cl$ (R = *p*- or *m*-tolyl), reported by Hiraki et al., which contains the six atoms of the chelate on a plane within 0.06 Å.[46]

(39) Treatment of **1** with CO_2 similarly affords $Ru(IMes)_2(CO)(\kappa^2\text{-}O_2COEt)H$, which has been characterized by ^1H and $^{13}C\{^1H\}$ NMR spectroscopy. ^1H NMR (C_6D_6, 400 MHz, 293 K): δ 6.84 (br s, 4H, $C_6H_2Me_3$), 6.80 (br s, 4H, $C_6H_2Me_3$), 6.14 (s, 4H, NC*H*=C*H*N), 3.57 (q, J_{HH} = 6.80 Hz, 2H, OCH_2), 2.27 (s, 12H, CH_3), 2.09 (s, 12H, CH_3), 2.05 (s, 12H, CH_3), 1.12 (t, J_{HH} = 6.80 Hz, 3H, OCH_2CH_3), −18.80 (s, 1H, Ru-H). $^{13}C\{^1H\}$ (C_6D_6, 293 K): δ 208.1 (s, Ru-*C*O), 194.1 (s, Ru-*C*), 158.7 (s, *C*-OH), 138.8 (s, N-*C*), 137.4 (s), 137.1 (s, *C*-*p*-CH_3), 136.2 (s, *C*-*o*-CH_3), 129.3 (s, *m*-*C*H), 129.0 (s, *m*-*C*H), 122.4 (s, N*C*H=*C*HN), 60.6 (s, OCH_2), 21.8 (s, *p*-CH_3), 19.2 (s, *o*-CH_3), 19.0 (s, *o*-CH_3), 15.9 (s, OCH_2CH_3).

(40) Nakamoto, K. *Infrared and Raman Spectra of Inorganic and Coordination Compounds*, 3rd ed.; Wiley: New York, 1978.

(41) (a) Ashworth, T. V.; Singleton, E. *J. Chem. Soc., Chem. Commun.* **1976**, 204. (b) Yoshida, T.; Thorn, D. L.; Okano, T.; Ibers, J. A.; Otsuka, S. *J. Am. Chem. Soc.* **1979**, *101*, 4212.

(42) Dobson, A.; Moore, D. S.; Robinson, S. D.; Hursthouse, M. B.; New, L. *Polyhedron* **1985**, *4*, 1119.

(43) Rotem, M.; Stein, Z.; Shvo, Y. *J. Organomet. Chem.* **1990**, *387*, 95.

(44) Dell'Amico, D. B.; Claderazzo, F.; Labella, L.; Marchetti, F. *J. Organomet. Chem.* **2000**, *596*, 144.

(45) McLoughlin, M. A.; Keder, N. L.; Harrison, W. T. A.; Flesher, R. J.; Mayer, H. A.; Kaska, W. C. *Inorg. Chem.* **1999**, *38*, 3223.

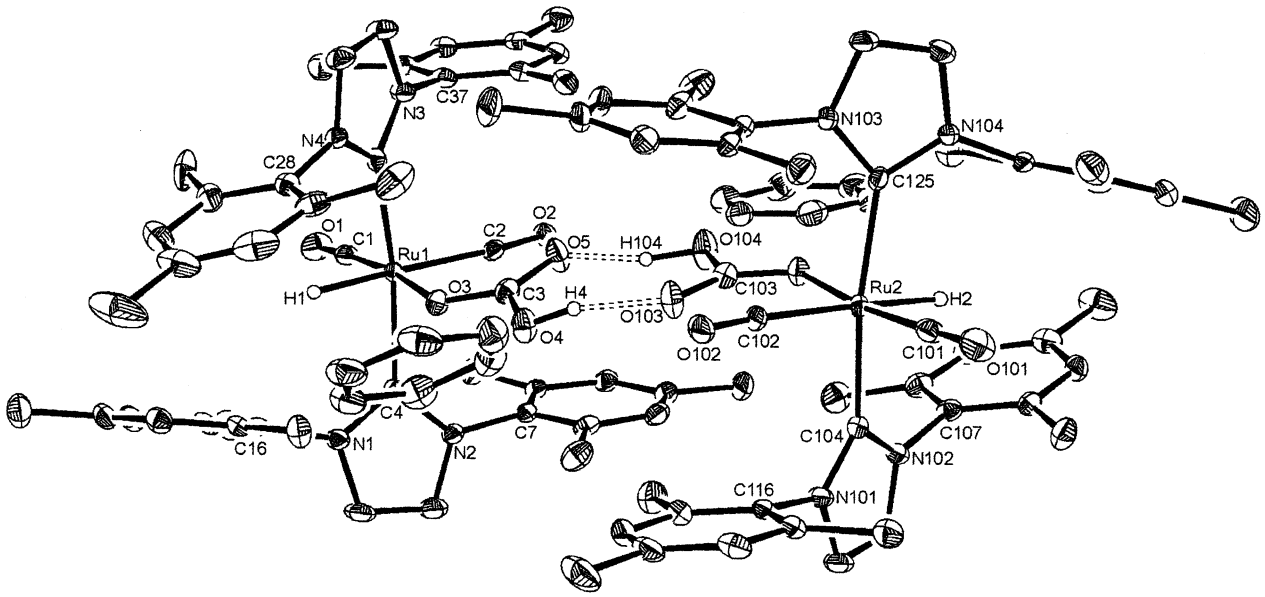

Figure 7. ORTEX diagram of $Ru(IMes)_2(CO)_2(OC(O)OH)H$ (**7**). Thermal ellipsoids are shown at the 30% probability level.

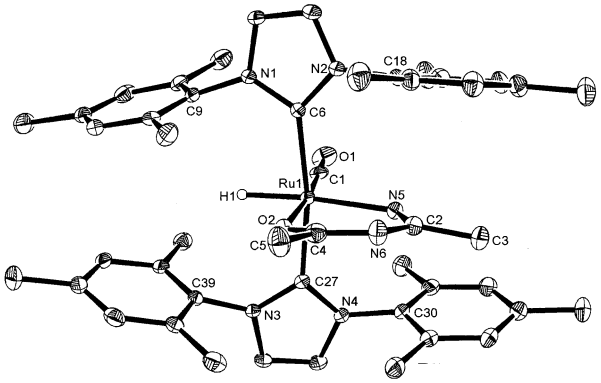

Figure 8. ORTEX diagram of $Ru(IMes)_2(CO)(NH{=}C(CH_3){-}N{=}C(CH_3)O)H$ (**12**). Thermal ellipsoids are shown at the 30% probability level.

Table 7. Selected Bond Lengths [Å] and Angles [deg] for $Ru(IMes)_2(CO)_2(\eta^1\text{-}OC(O)OH)H$ (7)

Ru(1)−C(1)	1.818(3)	Ru(1)−C(2)	1.989(3)
Ru(1)−C(25)	2.110(3)	Ru(1)−C(4)	2.116(3)
Ru(1)−O(3)	2.1344(18)	Ru(2)−C(101)	1.820(3)
Ru(2)−C(102)	1.982(3)	Ru(2)−C(125)	2.112(4)
Ru(2)−C(104)	2.119(3)	Ru(2)−O(103)	2.1352(19)
O(1)−C(1)	1.164(3)	O(2)−C(2)	1.133(4)
O(3)−C(3)	1.278(3)	O(4)−H(4)	0.91(5)
O(4)−C(3)	1.348(3)	O(5)−C(3)	1.231(4)
O(5)−H(104)	1.58(5)	O(101)−C(101)	1.150(3)
O(102)−C(102)	1.145(3)	O(103)−C(103)	1.268(3)
O(104)−H(104)	1.04(5)	O(104)−C(103)	1.341(4)
O(105)−C(103)	1.237(3)	O(105)−H(4)	1.74(5)

C(1)−Ru(1)−C(2)	93.08(13)	C(1)−Ru(1)−C(25)	95.33(13)
C(2)−Ru(1)−C(25)	94.53(13)	C(1)−Ru(1)−C(4)	90.82(13)
C(2)−Ru(1)−C(4)	96.73(12)	C(25)−Ru(1)−C(4)	166.85(12)
C(1)−Ru(1)−O(3)	171.69(11)	C(2)−Ru(1)−O(3)	94.52(10)
C(25)−Ru(1)−O(3)	87.43(10)	C(4)−Ru(1)−O(3)	84.94(10)
C(101)−Ru(2)−C(102)	94.89(14)	C(101)−Ru(2)−C(125)	89.48(13)
C(102)−Ru(2)−C(125)	97.78(12)	C(101)−Ru(2)−C(104)	93.12(13)
C(102)−Ru(2)−C(104)	94.02(12)	C(125)−Ru(2)−C(104)	167.66(12)
C(101)−Ru(2)−O(103)	170.19(12)	C(102)−Ru(2)−O(103)	94.71(10)
C(125)−Ru(2)−O(103)	87.22(10)	C(104)−Ru(2)−O(103)	88.22(10)
C(3)−O(3)−Ru(1)	125.23(19)	H(4)−O(4)−C(3)	106(3)

A comparison of bond lengths in the structures also reveals significant differences (Figure 9). Most noticeable is the lengthening of the Ru−O and Ru−N distances in **12**, and the fact that Ru−O is now shorter than the Ru−N distance. However, lengthening of the Ru−O bond length in **12** compared to the Hiraki complex would be expected due to the presence of hydride compared to chloride in the *trans* position.

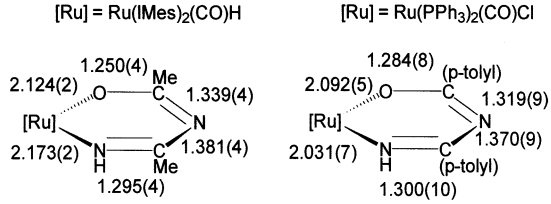

Figure 9. Comparison of bond lengths in the *N*-imidoyl-imidato complexes $Ru(IMes)_2(CO)(NH{=}C(CH_3){-}N{=}C(CH_3)O)H$ and $Ru(PPh_3)_2(CO)(NH{=}C(p\text{-tolyl}){-}N{=}C(p\text{-tolyl})O)Cl$.

Table 8. Selected Bond Lengths [Å] and Angles [deg] for $Ru(IMes)_2(CO)(NH{=}C(CH_3){-}N{=}C(CH_3)O)H$ (12)

Ru(1)−C(1)	1.828(3)	Ru(1)−C(27)	2.098(3)
Ru(1)−C(6)	2.107(3)	Ru(1)−O(2)	2.124(2)
Ru(1)−N(5)	2.173(2)	O(1)−C(1)	1.145(4)
O(2)−C(4)	1.250(4)	N(1)−C(6)	1.376(4)
N(1)−C(8)	1.385(4)	N(1)−C(9)	1.447(4)
N(2)−C(6)	1.376(4)	N(2)−C(7)	1.391(4)
N(2)−C(18)	1.442(4)	N(3)−C(27)	1.372(4)
N(3)−C(28)	1.391(4)	N(3)−C(39)	1.448(4)
N(4)−C(27)	1.373(4)	N(4)−C(29)	1.387(4)
N(4)−C(30)	1.447(4)	N(5)−C(2)	1.295(4)
N(6)−C(4)	1.339(4)	N(6)−C(2)	1.381(4)
C(2)−C(3)	1.506(4)	C(4)−C(5)	1.508(5)

C(1)−Ru(1)−C(27)	90.27(12)	C(1)−Ru(1)−C(6)	89.03(12)
C(27)−Ru(1)−C(6)	170.28(11)	C(1)−Ru(1)−O(2)	174.31(11)
C(27)−Ru(1)−O(2)	89.61(10)	C(6)−Ru(1)−O(2)	90.13(10)
C(1)−Ru(1)−N(5)	104.90(12)	C(27)−Ru(1)−N(5)	93.46(10)
C(6)−Ru(1)−N(5)	96.09(10)	O(2)−Ru(1)−N(5)	80.79(9)
C(4)−O(2)−Ru(1)	129.3(2)	C(2)−N(5)−Ru(1)	129.5(2)
C(4)−N(6)−C(2)	121.5(3)	O(1)−C(1)−Ru(1)	178.0(3)
N(5)−C(2)−N(6)	126.1(3)	N(5)−C(2)−C(3)	121.6(3)
N(6)−C(2)−C(3)	112.4(3)	O(2)−C(4)−N(6)	130.3(3)
O(2)−C(4)−C(5)	114.6(3)	N(6)−C(4)−C(5)	115.1(3)

The formation of $Ru(PPh_3)_2(CO)(NH{=}CRN{=}CRO)Cl$ is proposed to arise via nitrile hydration to give an

(46) Hiraki, K.; Kinoshita, Y.; Kinoshita-Kawashima, J.; Kawano, H. *J. Chem. Soc., Dalton Trans.* **1996**, 291. Hiraki, K.; Kinoshita, Y.; Ushiroda, H.; Koyama, S.; Kawano, H. *Chem. Lett.* **1997**, 1243.

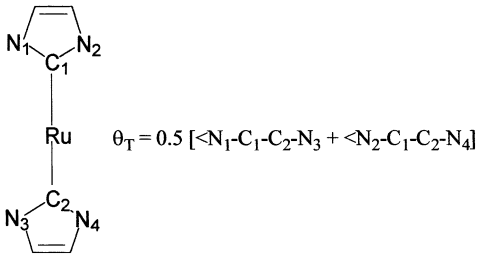

Figure 10. Twist angle (θ_T) in $Ru(IMes)_2$ complexes.

intermediate amidato complex, which subsequently inserts a second nitrile to give the final product following a 1,3-hydrogen shift. The presence of water is therefore vital to formation of the metallacyclic complex. Although we have not probed as yet the mechanism of formation of **12**, a similar process would seem reasonable due to the availability of water from **2**. Similar six-membered-ring oxa-aza metallacycles have been characterized for Zr, Ni, and Cu.[47−49]

Structural Comparisons of $Ru(IMes)_2$ Complexes. While there a number of structurally characterized bis-carbene complexes reported in the literature,[50] only very few of these contain two IMes ligands.[51] A comparison of the crystallographically determined structures reported herein reveals some noteworthy trends. In the first instance, the twist angle (θ_T) as defined in Figure 10 varies across all compounds, from 18° in the propanethiol complex **8** to 48° for the aqua complex **2**. This is not unexpected, as unfavorable interactions between the *para*-methyl substituents on the mesityl rings might result if θ_T had a value of zero. The magnitude of the twist angle appears to be inversely proportional to the steric demand of the varying equatorial ligand in the *trans* dihydride complexes, as θ_T for the propanethiol complex (**8**), the ethanol complex (**1**), and the aqua complex (**2**) are 18.2°, 32.3°, and 48.0°, respectively. The monohydride isonicotinate complex (**11**), with a comparable θ_T of 27.6°, also fits into this category of complexes, as the bulky equatorial ligands are oriented almost perpendicular to the carbene ring planes. On the face of it, this pattern would seem to be reversed for the bis-carbonyl complexes, where θ_T for the propanethiolate complex (**9**), the monodentate bicarbonate complex (**7**), and the hydroxy hydride species (**6**) are, correspondingly, 41.8°, 39.0°, and 22.8°, with the chelate (**12**) having a value of 26.4°. In some structures the proximity between an *ortho*-methyl carbon on the mesityl ring of one carbene to the centroid of the opposing aromatic ring on the second carbene might suggest the presence of some C−H···π stabilization, but this is a little tenuous given the inherent bulk of the carbenes themselves.

Throughout the dihydride complexes, the IMes fragments in the molecule tend to be approximately axial with respect to the equatorial plane of the molecule (as defined by the metal center, hydrides, and ligand atoms bound to the metal), and this is reflected in the $C_{carbene}$−Ru−$C_{carbene}$ angles for these compounds, which have values of 180° (**1**), 175.43(9)° (**2**), 177.56(4)° (**8**), and 178.82(8)° (**11**). Despite the inherent difficulty in locating hydrogen atoms from X-ray analysis, it is reasonable to say that the hydrides in all of these complexes are located in the two "pockets", on either side of the ruthenium, created by the IMes ligands, along a vector through the metal center that bisects θ_T.

Comparative $C_{carbene}$−Ru−$C_{carbene}$ angles for the bis-carbonyl complexes **6**, **7**, and **9** and the chelate compound **12** are considerably more acute at 167.94(8)°, 166.85(12)°, 165.91(6)°, and 170.28(11)°, respectively. This is inevitable, as one of the "pockets" has to expand to accommodate a substituent considerably larger than a hydride in these four compounds, which results in concomitant compression of the mesityl rings enfolding the hydride. Asymmetry in the $N_{carbene}$−$C_{carbene}$−Ru angles strongly reflects this intramolecular elasticity with typical decreases of 3° on the hydride side of a carbene compared with the alternative angle in the same carbene. It is also striking that, in these compounds, the pairs of aromatic rings that envelop individual pocketed coordination sites on the metal are almost mutually coplanar. Shortest distances between the carbons of one ring surrounding a carbonyl pocket and the least squares plane of the opposing ring are 5.53 Å (**12**), 5.72 Å (**6**), 6.08 Å (**7**), and 6.14 Å for **9**. Analysis of the superstructures for all compounds did not reveal any specific insight. Aromatic rings from neighboring molecules in the lattice of **1** appear to stack, but an average distance between the carbons of one ring and the least squares plane of the other of 4.3 Å suggests that this may largely be a packing effect.

Summary and Conclusions

Attempted crystallization of $Ru(IMes)_2(AsPh_3)(CO)H_2$ by ethanol or hexane led to the isolation of $Ru(IMes)_2(CO)(EtOH)H_2$ (**1**) and $Ru(IMes)_2(CO)(H_2O)H_2$ (**2**), respectively, both of which contain an unusual *trans* arrangement of the hydride ligands. Both of these compounds prove highly reactive toward a range of small molecules to afford Ru−X (X = heteroatom) complexes through either simple substitution processes (e.g., displacement of water by thiol) or more complex reactions to give monohydride $Ru(IMes)_2(CO)_2(X)H$ compounds. Within the latter group, $Ru(IMes)_2(CO)_2(OH)H$ (**6**) and $Ru(IMes)_2(CO)_2(\eta^1\text{-}O_2COH)H$ (**7**) are of particular interest in that they represent rare examples of fully characterized hydroxy hydride and monodentate bicarbonate complexes. In all of the cases we have studied, reaction of the Ru−HOR (R = H, Et) bond occurs in preference to chemistry at the Ru−H ligand.

Of particular interest to us at the outset of this work was the likely stability of the Ru−X bonds.[8b,52] Caulton

(47) Carney, M. J.; Walsh, P. J.; Hollander, F. J.; Bergman, R. G. *J. Am. Chem. Soc.* **1989**, *111*, 8751. Carney, M. J.; Walsh, P. J.; Hollander, F. J.; Bergman, R. G. *Organometallics* **1992**, *11*, 761.

(48) Vart, J. C. J.; Bassi, I. W.; Calcaterra, M.; Pieroni, M. *Inorg. Chim. Acta* **1978**, *28*, 201.

(49) Eberhardt, J. K.; Fröhlich, R.; Venne-Dunker, S.; Würthwein, E.-U. *Eur. J. Inorg. Chem.* **2000**, 1739.

(50) (a) Hitchcock, P. B.; Lappert, M. F.; Pye, P. L. *J. Chem. Soc., Chem. Commun.* **1976**, 644. (b) Hitchcock, P. B.; Lappert, M. F.; Pye, P. L. *J. Chem. Soc., Dalton Trans.* **1978**, 826. (c) Weskamp, T.; Schattenmann, W. C.; Spiegler, M.; Herrmann, W. A. *Angew. Chem., Int. Ed.* **1998**, *37*, 2490. (d) Chaumonnot, A.; Donnadieu, B.; Sabo-Etienne, S.; Chaudret, B.; Buron, C.; Bertrand, G.; Metivier, P. *Organometallics* **2001**, *20*, 5614. (e) Gründemann, S.; Albrecht, M.; Kovacevic, A.; Faller, J. W.; Crabtree, R. H. *J. Chem. Soc., Dalton Trans.* **2002**, 2163.

(51) Arduengo, A. J., III; Dias, H. V. R.; Calabrese, J. C.; Davidson, F. *Organometallics* **1993**, *12*, 3405. Arduengo, A. J., III; Gamper, S. F.; Calabrese, J. C.; Davidson, F. *J. Am. Chem. Soc.* **1994**, *116*, 4391.

(52) Poulton, J. T.; Sigalas, M. P.; Eisenstein, O.; Caulton, K. G. *Inorg. Chem.* **1993**, *32*, 5490.

has shown the propensity of the coordinatively saturated iridium heteratom complexes $Ir(P^tBu_2Ph)_2(CO)(X)H_2$ to reductively eliminate H−X upon addition of CO is highly dependent upon X.[25b] Thus, for X = OC(O)OR and SPh, the 18-electron complex is metastable in the presence of CO, ultimately losing phosphine and HX to give 16-electron $Ir(P^tBu_2Ph)(CO)_2H$. When X = F or OPh, HX loss is almost instantaneous. These patterns of reactivity are governed by the π-donating ability of X ($p\pi-d\pi$ interactions destabilize the 18-electron species and stabilize 16-electron complexes) and the strength of the H−X bond that is formed upon elimination. In the case of $Ru(IMes)_2(CO)_2(X)H$, we see some evidence for Ru−X reaction and elimination, though not via simple HX reductive elimination. Hence, while $Ru(IMes)_2(CO)_2(OH)H$ reacts with CO to give $Ru(IMes)_2(CO)_3$, the pathway involves a series of insertion and elmination processes leading to the final product. We might expect that removal of one (or both) CO ligand(s) from $Ru(IMes)_2(CO)_2(X)H$ would enhance the reactivity of the Ru−X bonds; we are actively working toward this at present.

In conclusion, the presence of two bulky IMes ligands on Ru has been shown to help stabilize bonds to oxygen, nitrogen, and sulfur ligands. Further work is in progress to fully examine the reactivity of these linkages and to try to extend the scope to include other X heteroatoms.

Experimental Section

General Comments. All manipulations were carried out using standard Schlenk, high-vacuum, and glovebox techniques. All solvents were distilled under a nitrogen atmosphere from purple solutions of sodium benzophenone ketyl (toluene, benzene, hexane, thf) or Mg/I_2 (ethanol, methanol). CH_3CN was dried over 3 Å molecular sieves and freeze−pump−thaw degassed. C_6D_6 and $C_6D_5CD_3$ (Goss Scientific Ltd.) were vacuum transferred from potassium/benzophenone. Propanethiol, HOC_6H_4-*p*-OEt, *p*-$HO_2CC_5H_4N$ (all Aldrich), CO (BOC, 99.9%), ^{13}CO (Promochem, 99%), and CO_2 (Aldrich) were used as received. $Ru(AsPh_3)_3(CO)H_2$ was prepared according to the literature.[53] IMes was prepared according to a modified route based on the method reported by Arduengo.[10b] ^1H NMR spectra were recorded on Bruker Avance 300 or Varian Mercury 400 MHz NMR spectrometers and referenced to the chemical shifts of residual protio solvent resonances (C_6D_5H δ 7.15, $C_6D_5CD_2H$ δ 2.10). $^{13}C\{^1H\}$ NMR spectra were referenced to C_6D_6 (δ 128.0) and $C_6D_5CH_3$ (δ 21.1). $^{31}P\{^1H\}$ NMR chemical shifts were referenced externally to 85% H_3PO_4 (δ 0.0). ^1H COSY, $^1H-^{13}C$ HMQC, and HMBC experiments were performed on the AVANCE spectrometer using standard Bruker pulse sequences. IR spectra were recorded as Nujol mulls on a Nicolet Protégé 460 FTIR spectrometer. Elemental analyses were performed at the University of Bath.

$Ru(IMes)_2(CO)(EtOH)H_2$ (1). An ampule fitted with a Teflon stopcock containing a solution of $Ru(AsPh_3)_3(CO)H_2$ (1.0 g, 0.95 mmol) in 20 mL of toluene and 3 equiv of IMes (0.87 g, 2.9 mmol) was heated at 75 °C for 4 days, during which time the solution turned deep red. The mixture was cooled to room temperature and evaporated to dryness, leaving an oily dark brown residue. Ethanol (10 mL) was added to give a brown solution, which was stirred for 2 h to give a yellow precipitate. This was filtered, washed with cold hexane (20 mL), and pumped to dryness to leave a yellow powder (0.51 g). A further batch of compound was isolated from the mother liquor. Total yield: 0.59 g, 78%. Anal. for $RuC_{45}H_{56}N_4O_2$ [found (calcd)]: C, 68.8 (68.75); H, 6.71 (7.18); N, 7.12 (7.13). ^1H NMR (C_6D_6, 400 MHz, 293 K): δ 6.85 (br s, 4H, $C_6H_2Me_3$), 6.83 (br s, 4H, $C_6H_2Me_3$), 6.20 (s, 4H, NC*H*=C*H*N), 3.81 (q, J_{HH} = 6.79 Hz, 2H, OCH_2), 2.35 (s, 12H, CH_3), 2.17 (s, 12H, CH_3), 2.09 (s, 12H, CH_3), 1.13 (t, J_{HH} = 6.69 Hz, 3H, OCH_2CH_3), −23.51 (s, 2H, Ru-H). $^{13}C\{^1H\}$ (C_6D_6, 293 K): δ 205.6 (s, Ru-*C*O), 197.9 (s, Ru-*C*), 138.2 (s, N-*C*), 137.0 (s, *C*-*p*-CH_3), 136.7 (s, *C*-*o*-CH_3), 136.6 (s, *C*-*o*-CH_3), 129.4 (s, *m*-*C*H), 129.3 (s, *m*-*C*H), 121.5 (s, NCH=*C*HN), 69.7 (s, OCH_2), 23.3 (s, OCH_2CH_3), 21.7 (s, *p*-CH_3), 19.2 (s, *o*-CH_3). IR (cm^{-1}): 1886 (ν_{CO}).

$Ru(IMes)_2(CO)(H_2O)H_2$ (2). Isolation of the aqua complex was performed as reported for **1**, but using a degassed mixture of hexane (20 mL) and water (5 mL) rather than ethanol. Yield: 0.58 g, 80%. Anal. for $RuC_{43}H_{52}N_4O_2$ [found (calcd)]: C, 68.7 (68.13); H, 6.49 (6.91); N, 7.44 (7.39). ^1H NMR (C_6D_6, 400 MHz, 293 K): δ 6.84 (br s, 4H, $C_6H_2Me_3$), 6.78 (br s, 4H, $C_6H_2Me_3$), 6.15 (s, 4H, NC*H*=C*H*N), 2.34 (s, 12H, CH_3), 2.18 (s, 12H, CH_3), 2.05 (s, 12H, CH_3), 0.93 (s, 2H, Ru-OH_2), −23.15 (s, 2H, Ru-H). $^{13}C\{^1H\}$ (C_6D_6, 293 K): δ 206.4 (s, Ru-*C*O), 198.6 (s, Ru-*C*), 138.1 (s, N-*C*), 137.2 (s, *C*-*p*-CH_3), 136.9 (s, *C*-*o*-CH_3), 136.5 (s, *C*-*o*-CH_3), 129.3 (s, *m*-*C*H), 129.2 (s, *m*-*C*H), 121.4 (s, NCH=*C*HN), 21.9 (s, *p*-CH_3), 19.2 (s, *o*-CH_3), 19.1 (s, *o*-CH_3). IR (cm^{-1}): 1861 (ν_{CO}), 1818 (ν_{Ru-H}).

$Ru(IMes)_2(CO)_2H_2$ (3). A toluene solution (2 mL) of **1** (0.20 g, 0.25 mmol) was heated at 90 °C for 2 weeks. The solution was then pumped to dryness, and 1 mL of hexane added. Stirring for 1 h afforded a creamy white precipitate. This was filtered off, washed with cold hexane (2 × 1 mL), and dried in vacuo. Yield: 0.13 g, 67%. Anal. for $RuC_{44}H_{50}N_4O_2$ [found (calcd)]: C, 68.5 (68.81); H, 6.28 (6.56); N, 7.20 (7.29). ^1H NMR (C_6D_6, 400 MHz, 293 K): δ 6.82 (s, 8H, $C_6H_2Me_3$), 6.12 (s, 4H, NC*H*=C*H*N), 2.21 (s, 12H, CH_3), 2.02 (s, 24H, CH_3), −6.53 (s, 2H, Ru-H). $^{13}C\{^1H\}$ (C_6D_6, 293 K): δ 204.3 (s, Ru-*C*O), 192.5 (s, Ru-*C*), 139.6 (s, N-*C*), 137.3 (s, *C*-*p*-CH_3), 136.3 (s, *C*-*o*-CH_3), 134.1 (s, *C*-*o*-CH_3), 128.9 (s, *m*-*C*H), 121.0 (s, NCH=*C*HN) 21.2 (s, *p*-CH_3), 18.6 (s, *o*-CH_3). IR (cm^{-1}): 1973 (ν_{CO}), 1936 (ν_{CO}).

$Ru(IMes)_2(CO)(HOC_6H_4$-*p*-OEt$)H_2$ (4). An ampule fitted with a Teflon stopcock containing a solution of $Ru(AsPh_3)_3(CO)H_2$ (0.50 g, 0.47 mmol) in 20 mL of toluene and 3 equiv of IMes (0.43 g, 1.5 mmol) was heated at 75 °C for 4 days, during which time the solution turned deep red. The mixture was cooled to room temperature and 1 equiv of HOC_6H_4-*p*-OEt (0.066 g, 0.47 mmol) added. The mixture was stirred for 1 h and then evaporated to dryness before addition of 10 mL of hexane. The compound crystallizes from a cold solution of hexane as a yellow microcrystalline solid. Yield: 0.31 g, 75%. Anal. for $RuC_{51}H_{60}N_4O_3$ [found (calcd)]: C, 70.4 (69.76); H, 6.80 (6.88); N, 5.52 (6.38). ^1H NMR (C_6D_6, 400 MHz, 293 K): δ 6.84 (br s, 4H, $C_6H_2Me_3$), 6.81 (br s, 4H, $C_6H_2Me_3$), 6.66 (br s, 2H, C_6H_4), 6.44 (br s, 2H, C_6H_4), 6.14 (s, 4H, NC*H*=C*H*N), 3.90 (br s, 2H, OCH_2), 2.36 (s, 12H, CH_3), 1.93 (s, 12H, CH_3), 1.90 (s, 12H, CH_3), 1.31 (br s, 3H, OCH_2CH_3), −24.48 (s, 1H, Ru-H). $^{13}C\{^1H\}$ (C_6D_6, 293 K): δ 205.5 (s, Ru-*C*O), 194.9 (s, Ru-*C*), 137.8 (s, N-*C*), 137.4 (s, *C*-*o*-CH_3), 136.9 (s, *C*-*o*-CH_3), 136.2 (s, *C*-*p*-CH_3), 129.5 (s, *m*-*C*H), 129.4 (s, *m*-*C*H), 121.9 (s, NCH=*C*HN), 116.0 (s, *o*/*m*-C_6H_4), 64.0 (br s, OCH_2), 21.6 (s, *p*-CH_3), 18.9 (s, *o*-CH_3), 15.5 (s, OCH_2CH_3). IR (cm^{-1}): 1881 (ν_{CO}).

$Ru(IMes)_2(CO)_3$ (5). Introduction of 1 atm of CO into a toluene solution (5 mL) of **2** (0.20 g, 0.25 mmol) gave a rapid color change from pale orange to colorless. The solution was left to stir with CO for a total of 5 days, during which time the solution became deep orange. Removal of the solvent under vacuo afforded an orange residue. This was dissolved in a minimum amount of toluene and layered with hexane to yield **5** as orange crystals (0.20 g, 99%). Anal. for $RuC_{45}H_{48}N_4O_3$ [found (calcd)]: C, 68.7 (68.72); H, 5.09 (5.13); N, 7.06 (7.13). ^1H NMR (C_6D_6, 400 MHz, 293 K): δ 6.78 (s, 8H, $C_6H_2Me_3$), 6.10 (s, 4H, NC*H*=C*H*N), 2.18 (s, 12H, CH_3), 2.05 (s, 24H, CH_3). $^{13}C\{^1H\}$ (C_6D_6, 293 K): δ 217.6 (s, Ru-*C*O), 186.8 (s, Ru-*C*), 138.9 (s, N-*C*), 137.9 (s, *C*-*p*-CH_3), 137.1 (s, *C*-*o*-CH_3), 129.5

(53) Harris, A. D.; Robinson, S. D. *Inorg. Chim. Acta* **1980**, *42*, 25.

(s, *m*-*C*H), 123.4 (s, NC*H*=*C*HN), 21.6 (s, *p*-*C*H$_3$), 19.1 (s, *o*-*C*H$_3$). IR (KBr, cm^{-1}): 1950, 1879, 1830 (ν_{CO}).

Ru(IMes)$_2$(CO)$_2$(OH)H (6). A toluene solution (5 mL) of **2** (0.20 g, 0.26 mmol) was stirred under 1 atm of carbon monoxide for 30 min, during which time the color changed from pale orange to colorless. The solution was concentrated (3 mL) and layered with hexane (10 mL). Colorless crystals were isolated from the hexane solution during the next 2 days. These were filtered off, washed with 2 × 10 mL of hexane, and dried in vacuo. Yield: 0.20 g, 95%. Anal. for $RuC_{44}H_{50}N_4O_3$ [found (calcd)]: C, 67.4 (67.41); H, 6.36 (6.43); N, 7.03 (7.14). ^{1}H NMR (C_6D_6, 400 MHz, 293 K): δ 6.75 (br s, 4H, C$_6$*H*$_2$Me$_3$), 6.74 (br s, 4H, C$_6$*H*$_2$Me$_3$), 6.08 (s, 4H, NC*H*=C*H*N), 2.19 (s, 24H, CH$_3$), 2.07 (s, 12H, CH$_3$), −3.75 (br s, 1H, Ru−OH), −4.27 (s, 1H, Ru-H). ^{13}C{^{1}H} (C_6D_6, 293 K): δ 204.2 (s, Ru-*C*O), 195.4 (s, Ru-*C*O), 184.8 (s, Ru-*C*), 139.7 (s, N-*C*), 137.8 (s, *C*-*p*-CH$_3$), 137.1 (s, *C*-*o*-CH$_3$), 137.0 (s, *C*-*o*-CH$_3$), 129.6 (s, *m*-*C*H), 129.3 (s, *m*-*C*H), 122.7 (s, NC*H*=*C*HN), 21.6 (s, *p*-*C*H$_3$), 19.0 (s, *o*-*C*H$_3$), 18.8 (s, CH$_3$). IR (cm^{-1}): 3426 (ν_{OH}), 2019 (ν_{CO}), 1880 (ν_{CO}), 1924 (ν_{Ru-H}).

Ru(IMes)$_2$(CO)$_2$(η^1-OC(O)OH)H (7). A toluene solution (5 mL) of Ru(IMes)$_2$(CO)$_2$(OH)H (0.20 g, 0.25 mmol) was stirred under 1 atm of carbon dioxide for 1 h at room temperature. The solution was then concentrated (3 mL) and layered with hexane (10 mL). Colorless crystals were formed from the hexane solution over the following 2 days. These were isolated, washed with 2 × 10 mL hexane, and dried in vacuo. Yield: 0.18 g, 86%. Anal. Calcd for $RuC_{45}H_{50}N_4O_5$ [found (calcd)]: C, 65.9 (65.28); H, 6.21 (6.09); N, 6.23 (6.77). ^{1}H NMR (C_6D_6, 400 MHz, 293 K): δ 12.10 (br s, 1H, OH), 6.87 (s, 4H, C$_6$*H*$_2$Me$_3$), 6.84 (s, 4H, C$_6$*H*$_2$Me$_3$), 6.09 (s, 4H, NC*H*=C*H*N), 2.27 (s, 12H, CH$_3$), 2.18 (s, 12H, CH$_3$), 2.14 (s, 12H, CH$_3$), −4.30 (s, 1H, Ru-H). ^{13}C{^{1}H} (C_6D_6, 293 K): δ 206.2 (s, Ru-*C*O), 194.8 (s, Ru-*C*O), 185.0 (s, Ru-*C*), 162.8 (s, O*C*(O)OH), 138.7 (s, N-*C*), 137.3 (s, *C*-*p*-CH$_3$), 136.7 (s, *C*-*o*-CH$_3$), 136.5 (s, *C*-*o*-CH$_3$), 129.3 (s, *m*-*C*H), 129.2 (s, *m*-*C*H), 122.9 (s, NC*H*=*C*HN), 21.6 (s, *p*-*C*H$_3$), 18.6 (s, *o*-*C*H$_3$), 18.5 (s, *p*-*C*H$_3$). IR (cm^{-1}): 2041 (ν_{CO}), 1965 (ν_{RuH}), 1916 (ν_{CO}), 1605 (ν_{OCO}), 1355 (ν_{OCO}).

Ru(IMes)$_2$(CO)(HSCH$_2$CH$_2$CH$_3$)H$_2$ (8). Two equivalents of propanethiol (60 μL, 0.76 mmol) was added to a toluene solution (5 mL) of **1** (0.30 g, 0.38 mmol) and the resulting solution stirred for 2 h. Removal of the solvent afforded a darkly colored residue, which was dissolved in a minimum amount of toluene and layered with hexane to afford deep red crystals of **8**. Yield: 0.13 g, 40%. The mother liquor was evaporated to dryness and washed with 2 × 5 mL of hexane at −60 °C and the precipitate dried in vacuo for 12 h. An additional crop of **8** was isolated as a microcystalline orange solid (0.13 g, total yield 83%). Anal. for $RuC_{46}H_{58}N_4OS$ [found (calcd)]: C, 68.0 (67.70); H, 6.77 (7.16); N, 6.83 (6.86). ^{1}H NMR (C_6D_6, 400 MHz, 293 K): δ 6.81 (br s, 4H, C$_6$*H*$_2$Me$_3$), 6.77 (br s, 4H, C$_6$*H*$_2$Me$_3$), 6.25 (s, 4H, NC*H*=C*H*N), 2.38 (t, 2H, J_{HH} = 7.20 Hz, SC*H*$_2$), 2.32 (s, 12H, CH$_3$), 2.12 (br m, 24H, CH$_3$), 1.60 (m, J_{HH} = 7.20 Hz, 2H, CH$_2$), 1.04 (t, J_{HH} = 7.20 Hz, 3H, CH$_2$C*H*$_3$), −23.77 (s, 2H, Ru-H). ^{13}C{^{1}H} (C_6D_6, 293 K): δ 203.1 (s, Ru-*C*O), 197.5 (s, Ru-*C*), 137.1 (s, N-*C*), 136.6 (s, *C*-*p*-CH$_3$), 136.2 (s, *C*-*o*-CH$_3$), 129.5 (s, *m*-*C*H), 122.3 (s, NC*H*=*C*HN), 38.7 (s, S*C*H$_2$), 30.1 (s, SCH$_2$*C*H$_2$), 21.9 (s, *p*-*C*H$_3$), 20.2 (br s, *o*-*C*H$_3$), 15.2 (s, SCH$_2$CH$_2$*C*H$_3$). IR (cm^{-1}): 1883 (ν_{CO}).

Ru(IMes)$_2$(CO)$_2$(SCH$_2$CH$_2$CH$_3$)H (9). A hexane solution (5 mL) of Ru(IMes)$_2$(CO)(HSCH$_2$CH$_2$CH$_3$)H$_2$ (0.10 g, 0.12 mmol) was stirred under 1 atm of CO for 30 min, during which time the color changed from pale orange to colorless followed by precipitation of a white powder. The solvent was removed via cannula, and the precipitate washed with 2 × 5 mL of cold hexane. The solid was then dissolved in a minimum amount of toluene and layered with hexane (10 mL). Colorless crystals were formed, which were isolated by filtration, washed with hexane (2 × 10 mL), and dried in vacuo. Yield: 0.10 g, 95%. Anal. for $RuC_{47}H_{56}N_4O_2S$ [found (calcd)]: C, 67.2 (67.03); H, 6.59 (6.70); N, 6.75 (6.65). ^{1}H NMR (C_6D_6, 400 MHz, 293 K): δ 6.78 (br s, 8H, C$_6$*H*$_2$Me$_3$), 6.07 (s, 4H, NC*H*=C*H*N), 2.19 (s, 12H, CH$_3$), 2.16 (t, 2H, J_{HH} = 7.60 Hz, SC*H*$_2$), 2.13 (s, 12H, CH$_3$), 2.12 (s, 12H, CH$_3$), 1.89 (sext, J_{HH} = 7.60 Hz, 2H, CH$_2$), 1.20 (t, J_{HH} = 7.60 Hz, 3H, CH$_2$C*H*$_3$), −4.10 (s, 1H, Ru-H). ^{13}C-{^{1}H} (C_6D_6, 293 K): δ 202.9 (s, Ru-*C*O), 199.0 (s, Ru-*C*O), 186.6 (s, Ru-*C*), 139.6 (s, N-*C*), 137.6 (s, *C*-*o*-CH$_3$), 137.2 (s, *C*-*o*-CH$_3$), 136.7 (s, *C*-*p*-CH$_3$), 129.7 (s, *m*-*C*H), 129.5 (s, *m*-*C*H), 123.3 (s, NC*H*=*C*HN), 38.9 (s, S*C*H$_2$), 30.4 (s, SCH$_2$*C*H$_2$), 21.8 (s, *p*-*C*H$_3$), 16.8 (s, *o*-*C*H$_3$), 16.5 (s, *o*-*C*H$_3$), 16.1 (s, SCH$_2$CH$_2$*C*H$_3$). IR (cm^{-1}): 2014 (ν_{CO}), 1946 (ν_{Ru-H}), 1896 (ν_{CO}).

Ru(IMes)$_2$(CO)(κ^2-O$_2$COH)H (10). A toluene solution (5 mL) of **2** (0.10 g, 0.13 mmol) was stirred under 1 atm of carbon dioxide for 1 h, during which the color changed from yellow to colorless. The solvent was removed under vacuo, and hexane (5 mL) was added. The resultant suspension was stirred at 0 °C to enforce precipitation of an off-white powder. This was filtered, washed with cold hexane (2 × 5 mL), and dried under vacuo. Yield: 0.08 g, 78%. Anal. for $RuC_{44}H_{50}N_4O_4$ [found (calcd)]: C, 66.3 (66.06); H, 6.39 (6.30); N, 7.01 (7.00). ^{1}H NMR (C_6D_6, 400 MHz, 293 K): δ 8.80 (br s, 1H, C-O*H*), 6.88 (br s, 4H, C$_6$*H*$_2$Me$_3$), 6.86 (br s, 4H, C$_6$*H*$_2$Me$_3$), 6.19 (s, 4H, NC*H*=C*H*N), 2.34 (s, 12H, CH$_3$), 2.14 (s, 12H, CH$_3$), 2.08 (s, 12H, CH$_3$), −20.73 (s, 1H, Ru-H). ^{13}C{^{1}H} (C_6D_6, 293 K): δ 207.4 (s, Ru-*C*O), 194.0 (s, Ru-*C*), 160.3 (s, *C*-OH), 138.3 (s, N-*C*), 137.2 (s, *C*-*o*-CH$_3$), 137.0 (s, *C*-*o*-CH$_3$), 136.5 (s, *C*-*p*-CH$_3$), 129.3 (s, *m*-*C*H), 129.2 (s, *m*-*C*H), 122.4 (s, NC*H*=*C*HN), 22.0 (s, *p*-*C*H$_3$), 19.3 (s, *o*-*C*H$_3$), 19.1 (s, *o*-*C*H$_3$). IR (cm^{-1}): 3416 (ν_{OH}), 1885 (ν_{CO}), 1593 (ν_{OCO}), 1453 (ν_{OCO}).

Ru(IMes)$_2$(CO)(κ^2-O$_2$CC$_5$H$_4$N)H (11). A toluene solution (5 mL) of **1** (0.20 g, 0.25 mmol) was stirred for 2 h at room temperature with 1 equiv of NC$_5$H$_4$CO$_2$H (0.030 g, 0.25 mmol). The solution was evaporated to dryness and the residue dissolved in a minimum amount of hexane. Slow concentration of the hexane solution afforded orange crystals (0.08 g) over 2 days. The remaining solution was cooled to −60 °C to enforce precipitation and yielded an additional 0.08 g as an orange powder. Yield: 83%. Multiple attempts to record CHN analysis for $RuC_{49}H_{53}N_5O_3$ consistently gave unacceptably high %C and %N content. ^{1}H NMR (C_6D_6, 400 MHz, 293 K): δ 8.70 (d, J_{HH} = 5.61 Hz, 2H, C$_5$H$_4$N), 7.44 (d, J_{HH} = 5.61 Hz, 2H, C$_5$H$_4$N), 6.87 (br s, 4H, C$_6$*H*$_2$Me$_3$), 6.68 (br s, 4H, C$_6$*H*$_2$Me$_3$), 6.11 (s, 4H, NC*H*=C*H*N), 2.28 (s, 12H, CH$_3$), 2.03 (s, 12H, CH$_3$), 1.88 (s, 12H, CH$_3$), −18.49 (s, 1H, Ru-H). ^{13}C{^{1}H} (C_6D_6, 293 K): δ 208.0 (s, Ru-*C*O), 193.0 (s, Ru-*C*), 172.3 (s, −O*C*O), 149.5 (s, C$_5$H$_4$N), 141.7 (s, C$_5$H$_4$N), 138.3 (s, N-*C*), 136.9 (s, *C*-*o*-CH$_3$), 136.7 (s, *C*-*o*-CH$_3$), 136.6 (s, *C*-*p*-CH$_3$), 129.0 (s, *m*-*C*H), 128.8 (s, *m*-*C*H), 123.5 (s, C$_5$H$_4$N), 122.0 (s, NC*H*=*C*HN), 21.2 (s, *p*-*C*H$_3$), 18.6 (s, *o*-*C*H$_3$), 18.4 (s, *o*-*C*H$_3$). IR (cm^{-1}): 1886 (ν_{CO}), 1596 (ν_{OCO}), 1461 (ν_{OCO}).

Ru(IMes)$_2$(CO)(NH=C(CH$_3$)N=C(CH$_3$)O)H (12). Acetonitrile (69 μL, 1.32 mmol) was added to a toluene solution (5 mL) of **2** (0.20 g, 0.26 mmol) and the mixture stirred for 6 days at room temperature. During this time the color changed from pale orange to off-yellow. Removal of the solvent and addition of cold hexane gave **12** as a white microcrystalline solid. Crystals suitable for X-ray diffraction were isolated from a concentrated solution of toluene layered with hexane. Yield: 0.20 g, 91%. Anal. for $RuC_{47}H_{56}N_6O_2$ [found (calcd)]: C, 67.2 (67.36); H, 6.97 (6.74); N, 9.38 (10.03). ^{1}H NMR (C_6D_6, 400 MHz, 293 K): δ 6.79 (s, 8H, C$_6$*H*$_2$Me$_3$), 6.08 (s, 4H, NC*H*=C*H*N), 5.73 (s, 1H, NH), 2.27 (s, 6H, CH$_3$), 2.15 (s, 12H, CH$_3$), 2.03 (s, 12H, CH$_3$), 1.99 (s, 3H, N=CC*H*$_3$), 1.52 (s, 3H, N=CC*H*$_3$), −11.40 (s, 1H, Ru-H). ^{13}C{^{1}H} (C_6D_6, 293 K): δ 210.3 (s, Ru-*C*O), 191.4 (s, Ru-*C*), 173.8 (s, O=*C*CH$_3$), 166.0 (s, NH=*C*CH$_3$), 139.0 (s, N-*C*), 136.6 (s, *C*-*o*-CH$_3$), 136.1 (s, *C*-*p*-CH$_3$), 128.9 (s, *m*-*C*H), 128.8 (s, *m*-*C*H), 122.2 (s, NC*H*=*C*HN), 31.6 (s, NH=CCH$_3$), 28.2 (s, O=CCH$_3$), 21.4 (s, *p*-*C*H$_3$), 18.8 (s, *o*-*C*H$_3$), 18.7 (s, *o*-*C*H$_3$). IR (cm^{-1}): 1865 (ν_{CO}), 2016 (ν_{Ru-H}).

X-ray Experimental Data. Crystallographic data for compounds **1**, **2**, **6**, **7**, **8**, **9**, **11**, and **12** are summarized in Table 9. Data were collected on a Nonius KappaCCD diffractometer

Table 9. Crystal Data and Structure Refinement for Compounds 1, 2, 6, 7, 8, 9, 11, and 12

	1	**2**	**6**	**7**
empirical formula	$C_{45}H_{56}N_4O_2Ru$	$C_{43}H_{52}N_4O_2Ru$	$C_{44}H_{50}N_4O_3Ru$	$C_{51}H_{56}N_4O_5Ru$
fw	786.00	757.96	783.95	906.07
T/K	150(2) K	150(2)	100(2)	150(2)
cryst syst	monoclinic	monoclinic	monoclinic	orthorhombic
space group	*C*2/*c*	*Pbca*	$P2_1/a$	$Pc2_1n$
a/Å	14.7320(2)	17.1940(2)	18.6240(2)	14.6284(1)
b/Å	17.8590(3)	19.3610(2)	10.7880(1)	18.9827(2)
c/Å	15.6780(2)	23.1920(2)	20.8450(2)	33.4047(4)
α/deg				
β/deg	91.839(1)		108.802(1)	
γ/deg				
U/Å^3	4122.74(10)	7720.46(14)	3964.60(7)	9276.04(16)
Z	4	8	4	8
D_c/g cm^{-3}	1.265	1.304	1.313	1.298
μ/mm^{-1}	0.421	0.447	0.439	0.388
F(000)	1656	3184	1640	3792
cryst size/mm	0.40 × 0.35 × 0.33	0.14 × 0.11 × 0.11	0.50 × 0.40 × 0.20	0.20 × 0.20 × 0.13
θ range for data collection/^{o}	3.69 to 25.03	3.51 to 27.49	3.73 to 27.48	3.52 to 27.48
index ranges	$-17 \le h \le 17$; $-21 \le k \le 21$; $-18 \le l \le 18$	$-22 \le h \le 21$; $-25 \le k \le 25$; $-30 \le l \le 30$	$-23 \le h \le 24$; $-13 \le k \le 14$; $-27 \le l \le 27$	$-18 \le h \le 18$; $-24 \le k \le 24$; $-43 \le l \le 43$
no. of reflns collected	30 043	111 187	59 593	44 812
no. of ind reflns	3601 [*R*(int) = 0.0356]	8832 [*R*(int) = 0.0775]	9018 [*R*(int) = 0.0437]	16261 [*R*(int) = 0.0409]
no. of reflns obsd ($I>2\sigma(I)$)	3566	6279	7741	13338
no. of data/restraints/ params	3601/1/269	8832/5/471	9018/2/516	16 261/3/1139
goodness-of-fit on F^2	1.376	1.010	1.066	0.986
final R1, wR2 indices [$I>2\sigma(I)$]	0.0417, 0.1267	0.0367, 0.0835	0.0381, 0.0938	0.0366, 0.0704
final R1, wR2 indices (all data)	0.0420, 0.1269	0.0656, 0.0962	0.0475, 0.0987	0.0528, 0.0747
largest diff peak and hole/ e Å^{-3}	0.804, −0.617	0.472, −0.530	1.225, −0.786	0.407, −0.493

	8	**9**	**11**	**12**
empirical formula	$C_{46}H_{58}N_4ORuS$	$C_{47}H_{56}N_4O_2RuS$	$C_{49}H_{53}N_5O_3Ru$	$C_{47}H_{56}N_6O_2Ru$
fw	816.09	842.09	861.03	838.05
T/K	150(2)	150(2)	150(2)	150(2)
cryst syst	monoclinic	monoclinic	monoclinic	monoclinic
space group	$P2_1/c$	$P2_1/c$	$P2_1/c$	$P2_1/n$
a/Å	14.6840(1)	11.7450(1)	a11.0830(2)	14.7840(2)
b/Å	12.3690(1)	15.3310(1)	b12.7380(2)	18.4460(3)
c/Å	23.2970(2)	25.2050(2)	c31.7490(5)	16.4750(2)
α/deg				
β/deg	101.425(1)	101.755(1)	96.001(1)	102.884(1)
γ/deg				
U/Å^3	4147.50(6)	4443.29(6)	4457.61(13)	4379.71(11)
Z	4	4	4	4
D_c/g cm^{-3}	1.307	1.259	1.283	1.271
μ/mm^{-1}	0.468	0.440	0.398	0.402
F(000)	1720	1768	1804	1760
cryst size/mm	0.50 × 0.50 × 0.50	0.20 × 0.20 × 0.10	0.25 × 0.15 × 0.15	0.25 × 0.10 × 0.05
θ range for data collection/^{o}	3.54 to 33.13	3.54 to 30.04	3.60 to 27.45	3.05 to 27.57
index ranges	$-22 \le h \le 22$; $-19 \le k \le 19$; $-35 \le l \le 35$	$-16 \le h \le 16$; $-21 \le k \le 21$; $-35 \le l \le 35$	$-12 \le h \le 14$; $-16 \le k \le 15$; $-40 \le l \le 41$	$-19 \le h \le 19$; $-23 \le k \le 23$; $-21 \le l \le 21$
no. of reflns collected	88 665	99 737	65 830	83 967
no. of ind reflns	15738 [*R*(int) = 0.0520]	12979 [*R*(int) = 0.0806]	10162 [*R*(int) = 0.0473]	10035 [*R*(int) = 0.0915]
no. of reflns obsd ($I>2\sigma(I)$)	13 131	10 375	8188	7511
no. of data/restraints/ params	15 738/2/508	12 979/1/513	10 162/0/553	10 035/2/526
goodness-of-fit on F^2	1.041	1.004	1.004	1.055
final R1, wR2 indices [$I>2\sigma(I)$]	0.0298, 0.0738	0.0339, 0.0813	0.0342, 0.0793	0.0487, 0.1008
final R1, wR2 indices (all data)	0.0412, 0.0795	0.0503, 0.0892	0.0504, 0.0851	0.0777, 0.1132
largest diff peak and hole/ e Å^{-3}	0.377, −0.727	0.629, −1.131	0.443, −0.544	2.536, −0.874

throughout. Full matrix anisotropic refinement was implemented in the final least squares cycles for all structures. All data were corrected for Lorentz and polarization. An absorption correction (multiscan) was applied to data for **2**, **6**, **7**, **8**, **9**, and **12** (maximum, minimum transmission factors were 0.95 0.88, 0.95 0.89, 0.95 0.93, 1.15 0.91, 0.96 0.82 and 0.98 0.87, respectively). Hydrogen atoms were included at calculated positions throughout with the exceptions of those specifically mentioned below.

In **1**, the asymmetric unit consisted of a half of one molecule with central ruthenium seated on a crystallographic 2-fold rotation axis. Hence, both the bound ethanol and carbonyl

group are positionally disordered about this axis in a 1:1 ratio. The alternative space group (*Cc*) was tested for this structure but was not viable, as the disorder was still present and convergence was very adversely affected. The hydride hydrogen in this structure was located and refined at distance of 1.6 Å from the parent atom [H−Ru−H 145(4)°]. Unfortunately, the alcoholic hydrogen could not be reliably located and thus was omitted from refinement. Disorder in the methyl groups based on C11 and C21 was also modeled in the final least squares cycles.

The hydrides in **2** were also located with only moderate confidence and were refined subject to distance restraints from the transition metal, from each other, and from the carbonyl carbon, C43. However, the hydrogen atoms on the bound water could not be located with any certainty and, hence, are omitted from refinement. Disorder also prevailed in **6** where the hydroxyl and *trans* carbonyl moieties are modeled at 70:30 occupancy and vice versa over the two sites. Nonetheless, the hydride and hydroxyl hydrogens in the major component of this structure were located and refined, with the former at a fixed distance of 1.6 Å from the metal center.

The structure of **7** was seen to contain two molecules in the asymmetric unit along with a pair of benzenes. The hydride and bicarbonate hydrogen atoms were readily located and refined, the former treated in a manner similar to that in compound **1**. In **8**, disorder was manifested in the sulfur atom between S1/S1A in a 68:32 ratio. Hydrides in **8** were located and refined at distance of 1.6 Å from the ruthenium atom, although the ADP for H2 is larger than desirable (possibly due to the sulfur disorder). However, the hydrogen attached to the sulfur atom could not be reliably located and hence was omitted from refinement. The carbonyl group in **11** was also disordered in a 60:40 ratio between C1/O1 and C1A/O1A, respectively. The methyl group attached to C45 in **12** exhibited disorder which was successfully accounted for in the refinement. H1 (attached to the metal) and H5 (attached to N5) were easily located in the penultimate electron density map and refined at fixed distances (1.6 and 0.89 Å, respectively) from the relevant parent atoms.

All structures were solved using SHELXS-97 and refined using SHELXL-97.[54] Crystallographic data for the structural analyses have been deposited with the Cambridge Crystallographic Data Centre, CCDC no. 191363 for compound **1**, 191364 for compound **2,** 191365 for compound **6**, 191366 for compound **7**, 191367 for compound **8**, 191368 for compound **9**, 191369 for compound **11**, and 191370 for compound **12**.

Acknowledgment. We acknowledge EPSRC for a project studentship (R.F.R.J.), the University of Bath for financial support, and Johnson Matthey plc for the loan of $RuCl_3$. EPSRC/JREI are thanked for funding the X-ray diffractometer.

Supporting Information Available: X-ray crystallographic data including tables of atomic coordinates, bond lengths and angles, anisotropic displacement parameters, hydrogen coordinates, and U_{eq}, and packing diagrams. This material is available free of charge via the Internet at http://pubs.acs.org.

OM020684E

(54) Sheldrick, G. M. *Acta Crystallogr.* **1990**, *467−473*, A46. Sheldrick, G. M. *SHELXL-97*, a computer program for crystal structure refinement; University of Göttingen, 1997.